

## CHAPTER IV

### RESULTS & DISCUSSION

We have investigated the rheological and optical properties of emulsions in terms of aging time, fatty alcohol concentration, temperature, and pH. The systems studied were

#### 4.1 Effect of Aging Time

Systems	Conditions
Miranol Ultra C32 : Fatty Alcohol = 1 : 2 %	Temperature = 26 <sup>0</sup> C pH = 8.7 - 9.2
Miranol Ultra C32 : Fatty Alcohol = 1 : 4 %	
Miranol Ultra C32 : Fatty Alcohol = 1 : 6 %	
Miranol Ultra C32 : Fatty Alcohol = 1 : 8 %	

#### 4.2 Effect of Fatty Alcohol Concentration

Systems	Conditions
Miranol Ultra C32 : Fatty Alcohol = 1 : 2 %	Temperature = 26 <sup>0</sup> C pH = 8.7- 9.2
Miranol Ultra C32 : Fatty Alcohol = 1 : 4 %	
Miranol Ultra C32 : Fatty Alcohol = 1 : 6 %	
Miranol Ultra C32 : Fatty Alcohol = 1 : 8 %	

#### 4.3 Effect of Temperature

Systems	Conditions
Miranol Ultra C32 : Fatty Alcohol = 1 : 2 %	Temperature = 26,35,55 <sup>0</sup> C pH = 8.7-9.2
Miranol Ultra C32 : Fatty Alcohol = 1 : 4 %	
Miranol Ultra C32 : Fatty Alcohol = 1 : 6 %	
Miranol Ultra C32 : Fatty Alcohol = 1 : 8 %	

#### 4.4 Effect of pH

Systems	Conditions
Miranol Ultra C32 : Fatty Alcohol = 1 : 2 %	Temperature = 26 <sup>0</sup> C pH = 5, 7, 8.7-9.2, 10
Miranol Ultra C32 : Fatty Alcohol = 1 : 4 %	
Miranol Ultra C32 : Fatty Alcohol = 1 : 6 %	
Miranol Ultra C32 : Fatty Alcohol = 1 : 8 %	

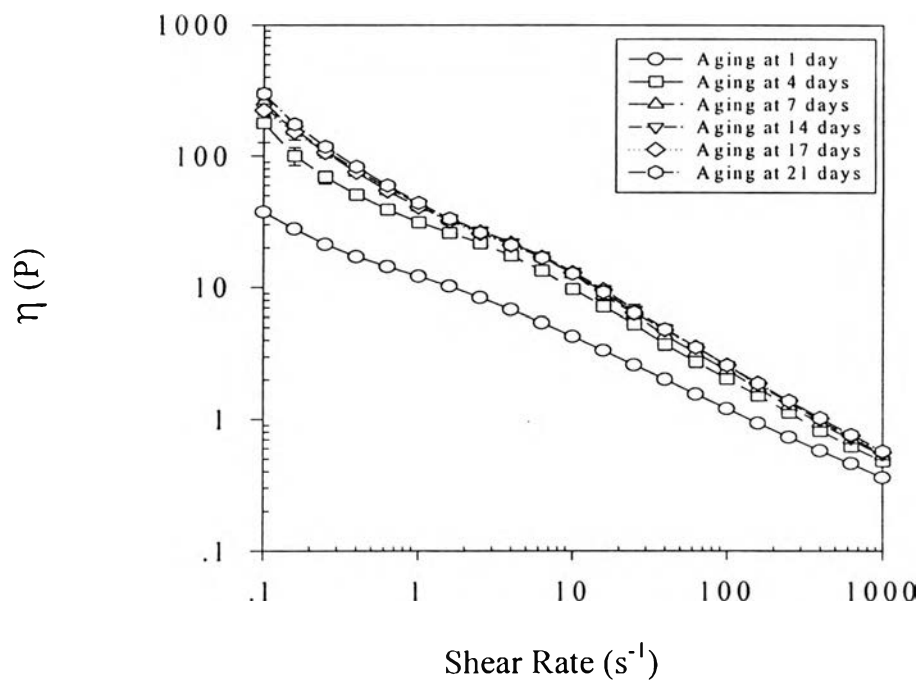
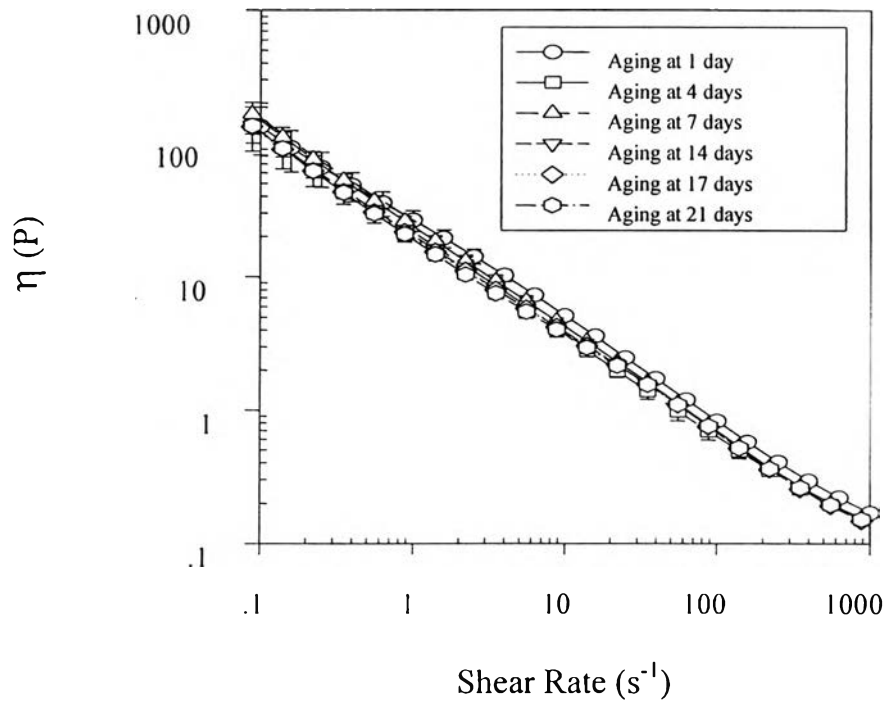
#### 4.1 Effect of Aging Time on Emulsion Structure

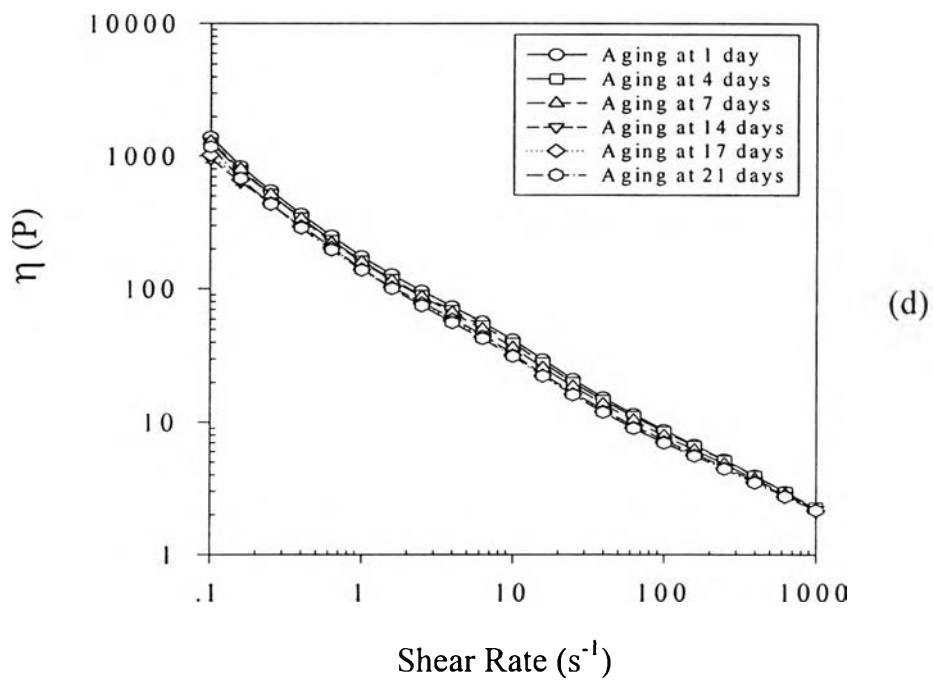
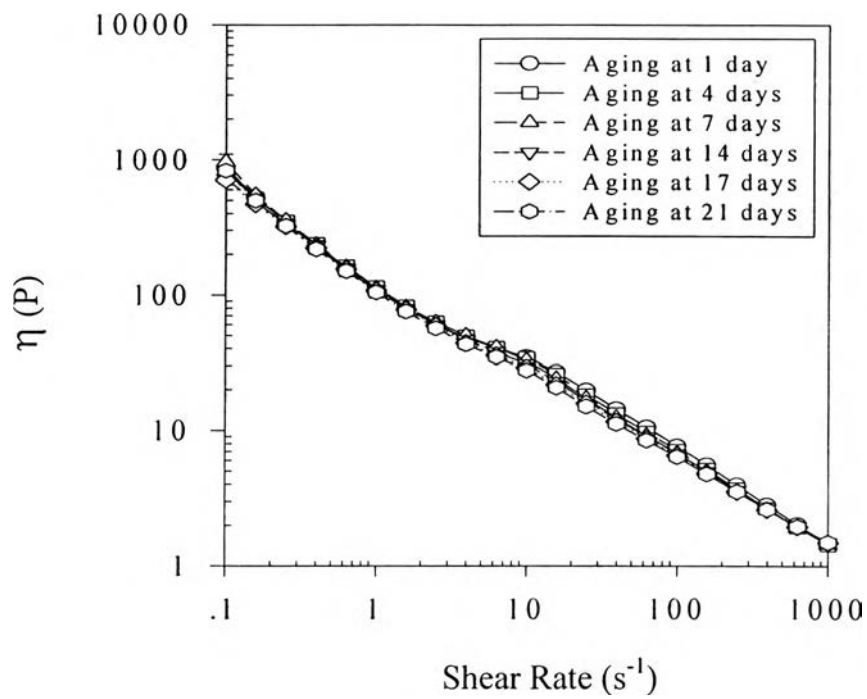
##### 4.1.1 Rheological Measurement

We investigated Miranol Ultra C32 with Fatty Alcohol emulsions at the following concentrations; MUC32 : FA = 1 : 2 , 1 : 4 , 1 : 6 and 1 : 8 % by weight.

##### *4.1.1.1 Viscosity as a Function of Aging Time*

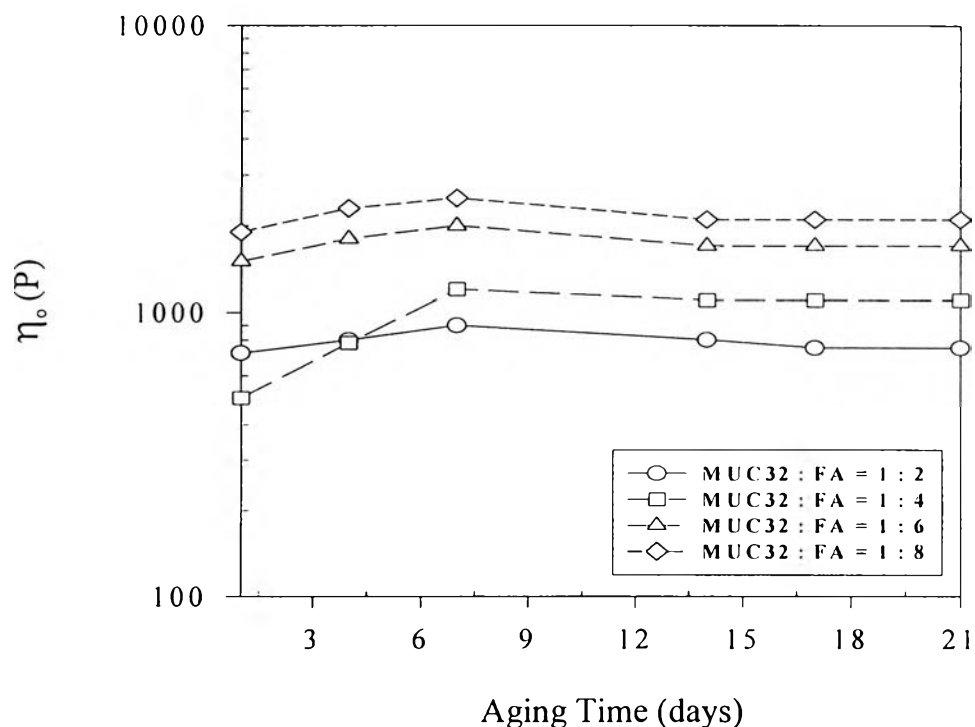
Figure 4.1 shows the viscosity of the emulsion systems against shear rate as a function of aging time. The viscosity profiles show a pronounced pseudoplastic or shear-thinning behavior. For the emulsions with MUC32:FA=1:2% by weight, viscosity did not show significant changes with aging time between 1 day to 21 days. Similarly, for the emulsions with MUC32:FA=1:6 and 1:8% by weight, the viscosity did not change significantly with aging time. At the fatty alcohol concentration ratio of 4% by weight, viscosity at any shear rate increased with aging time and reached the equilibrium after approximately 14 days.





**Figure 4.1** Viscosity against shear rate as a function of aging time: MUC32:FA = 1:2; (b) MUC32:FA = 1:4; MUC32:FA = 1:6; (d) MUC32:FA = 1:8, temperature was equal to  $26 \pm 1^{\circ}\text{C}$ , strain was 0.2% and pH was between 8.7 – 9.2.

#### 4.1.1.2 Zero Shear Viscosity

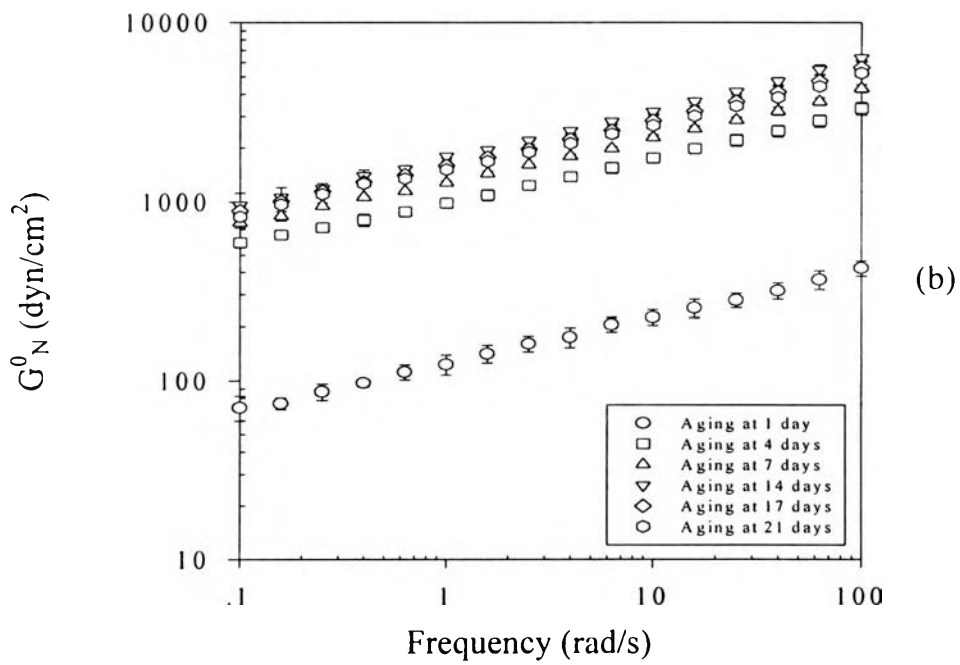
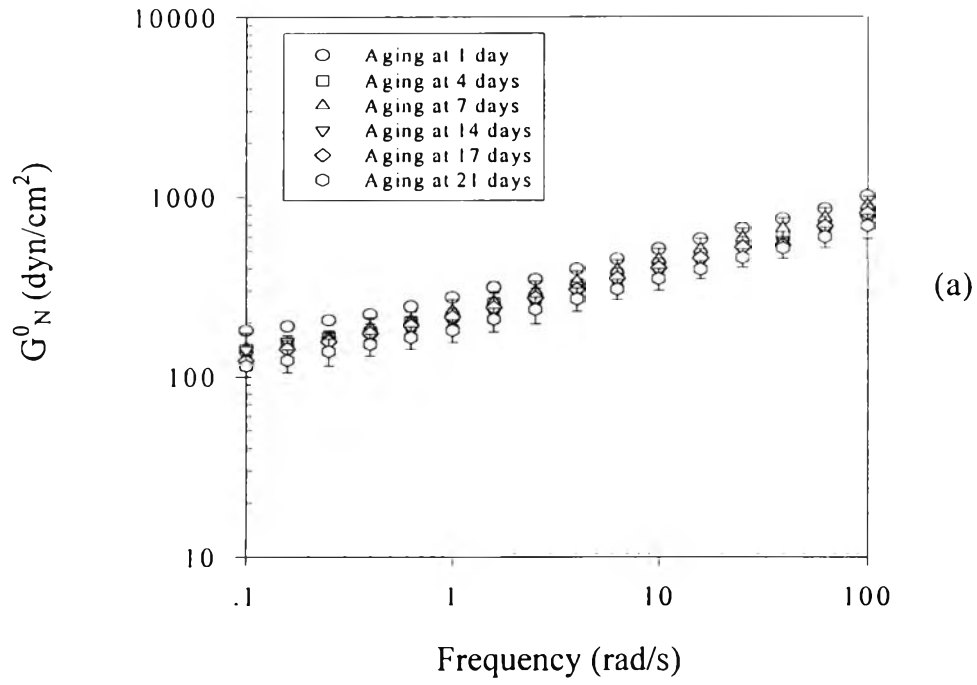


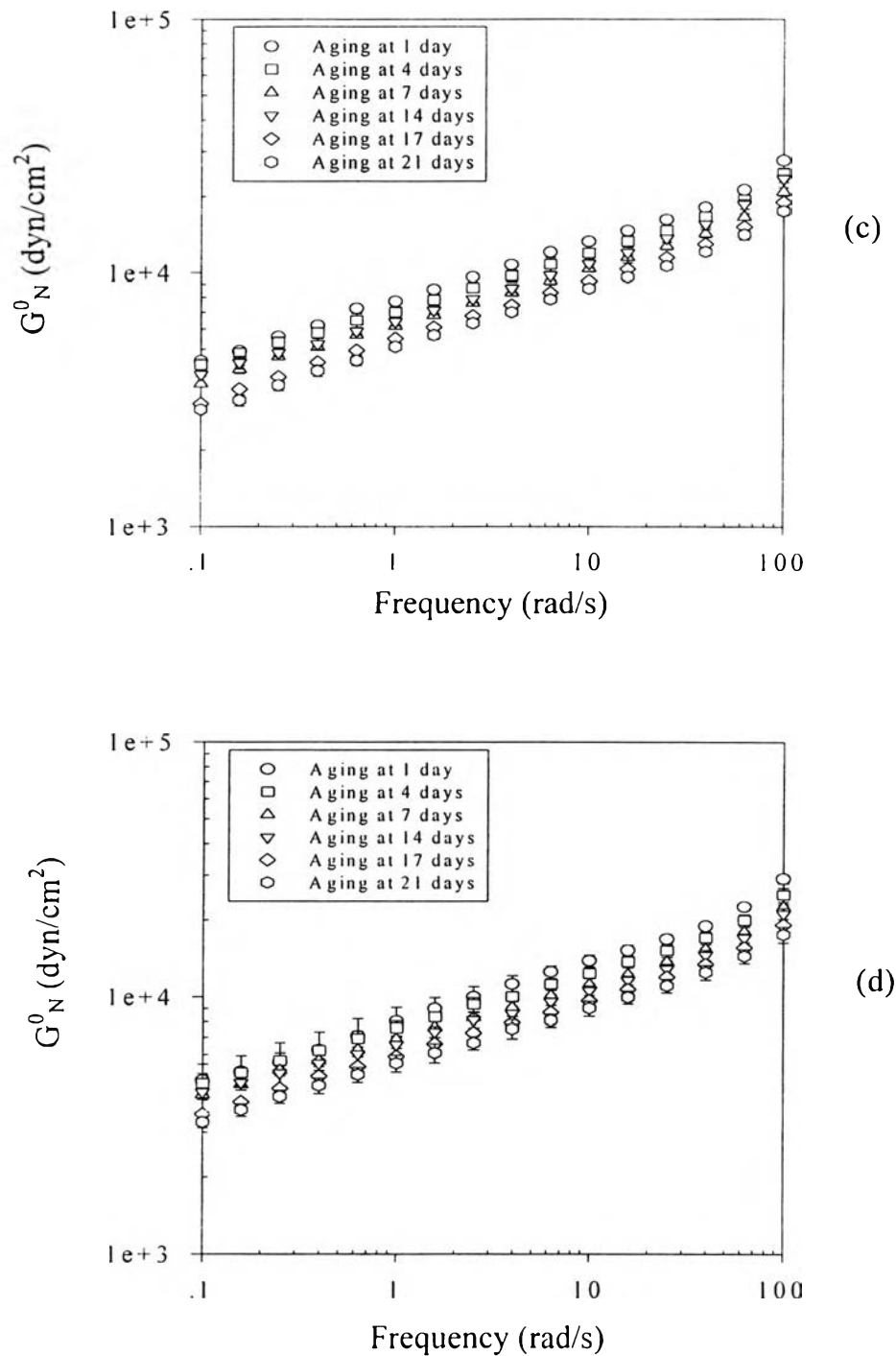
**Figure 4.2** Zero shear viscosity ( $\eta_0$ ) against aging time of various emulsions;  $\eta_0$  was  $\eta$  at shear rate  $0.01 \text{ s}^{-1}$ , temperature was equal to  $26 \pm 1^\circ\text{C}$ , and pH was between 8.7-9.2.

Figure 4.2 shows the zero shear viscosity ( $\eta_0$ ) against the number of aging days. Zero shear viscosity is defined as the viscosity at the shear rate of  $0.01 \text{ s}^{-1}$ . It can be seen that, for the emulsions with MUC32:FA=1:4% by weight, the zero shear viscosity ( $\eta_0$ ) increased as the sample was aged.

#### *4.1.1.3 Storage Modulus as a Function of Aging Time*

Figure 4.3 shows the double logarithmic plot of frequency-dependent storage modulus of surfactant and fatty alcohol mixtures as a function of aging time at the temperature of  $26 \pm 1^{\circ}\text{C}$ . For the emulsions with MUC32:FA=1:2, 1:6 and 1:8 % by weight, the storage modulus decreased at every frequencies after aging time of 1 day. This implies that the emulsions changed from a viscous or liquid like behavior to a solid-like behavior and the system possibly reached an equilibrium after aging 1 day. For the emulsion with MUC32:FA=1:4% by weight, the storage modulus increased at every frequencies with aging time until the aging time was 14 days. The storage modulus at aging 17 days was slightly smaller than that from aging 14 days. Data suggest that the system possibly reached an equilibrium after aging 14 days.





**Figure 4.3** Storage modulus against shear rate as a function of aging time: (a) MUC32:FA=1:2; (b) MUC32:FA=1:4; (c) MUC32:FA=1:6; (d) MUC32:FA = 1:8, and temperature was equal to  $26 \pm 1^\circ\text{C}$ , strain was 0.2%, and pH was between 8.7 – 9.2.



#### 4.1.1.4 Entanglement Storage Modulus

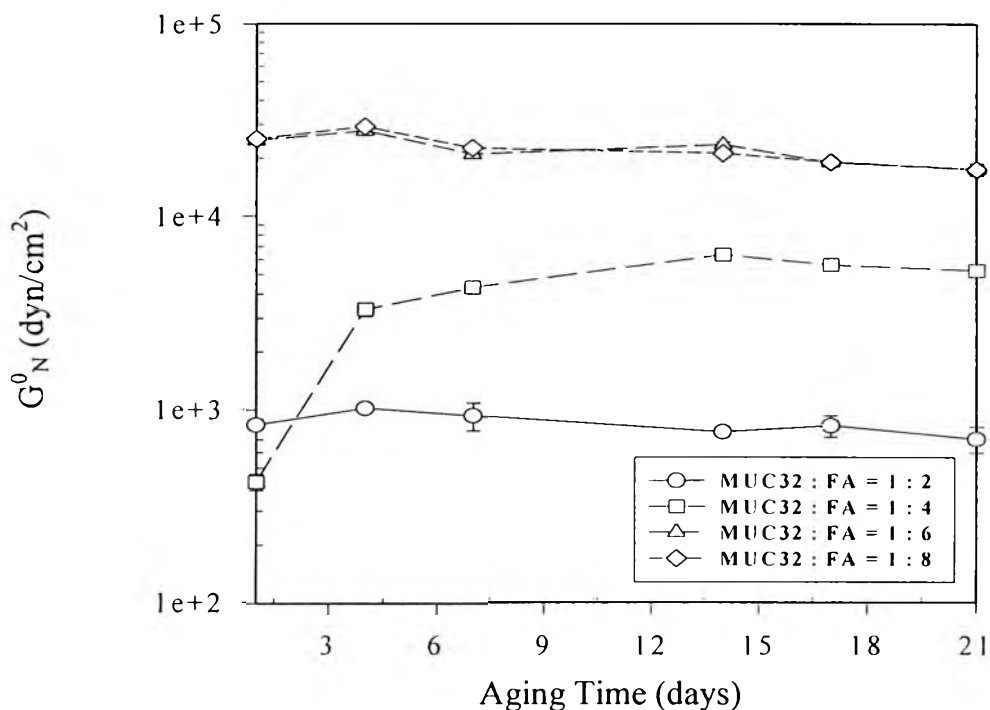


**Figure 4.4** Entanglement storage modulus ( $G_N^0$ ) against aging time of various concentration;  $G_N^0$  was  $G'$  at 100 rad/s, temperature was  $26 \pm 1^\circ\text{C}$ , strain was 0.2%, and pH was between 8.7-9.2.

Figure 4.4 shows  $G_N^0$  which is defined as  $G'(\omega)$  at 100 rad/s. It is referred to as the liquid-like entanglement storage modulus and it gives a measure of material rigidity or elasticity. For the emulsions with MUC32:FA=1:2, 1:6 and 1:8% by weight,  $G_N^0$  were nearly constant after the aging time of 1 day. Data suggest that the systems reached an equilibrium after 1 day. For the emulsion with MUC32:FA=1:4% by weight,  $G_N^0$  increased with aging time until the aging time was 14 days. After 14 days  $G_N^0$  slightly decreased and became constant. Data suggest that the system reached an equilibrium after 14 days.

#### 4.1.1.5 Bingham Stress

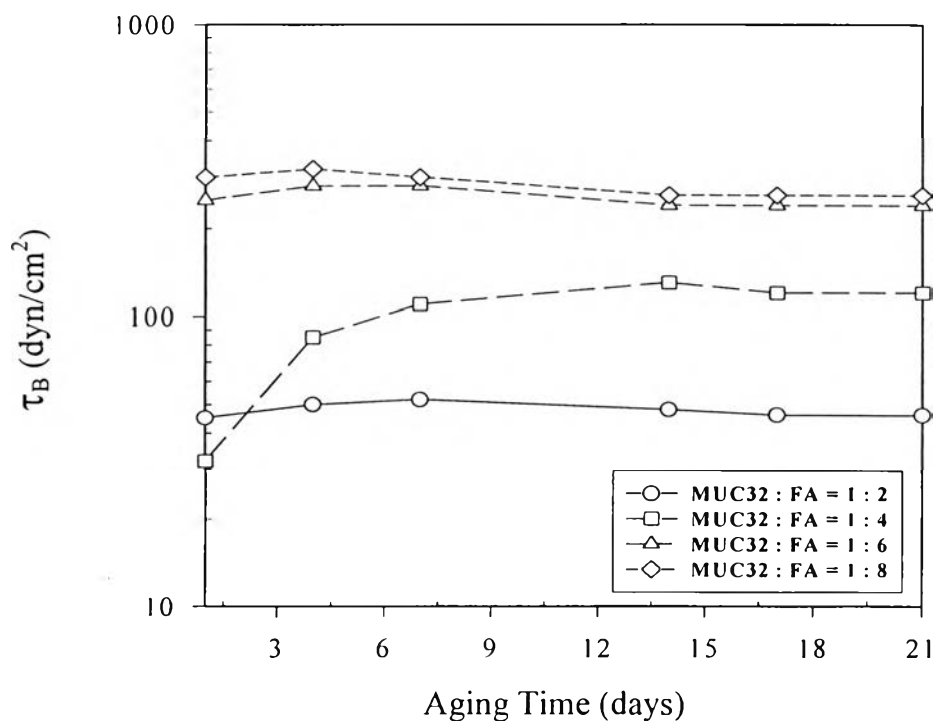
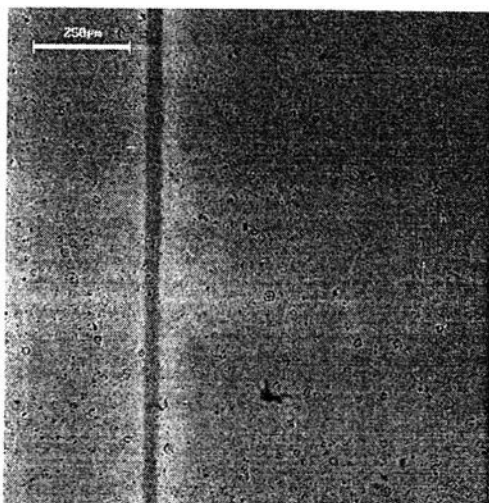


**Figure 4.5** Bingham stress ( $\tau_B$ ) against aging time of various emulsions; temperature was  $26 \pm 1^\circ\text{C}$ , and pH was between 8.7-9.2.

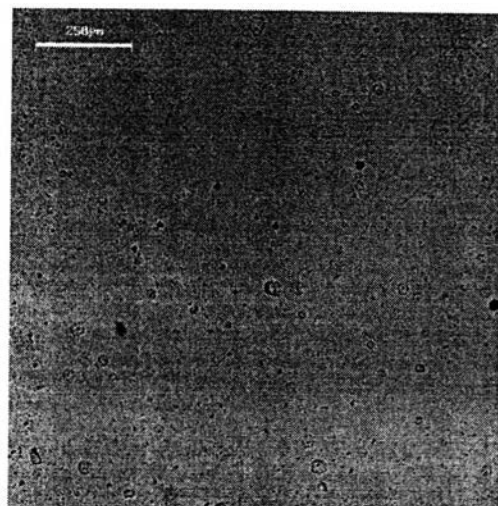
Figure 4.5 shows the  $\tau_B$  versus aging time.  $\tau_B$  is the yield stress which was obtained from a plot of the stress versus shear rate in the limit of zero shear rate. The plot shows the same behavior as the shear entanglement modulus. For the emulsions with surfactant and fatty alcohol ratios of 1 to 2, 6 and 8% by weight, the force or stress required to initiate the flow remained constant with aging time after 1 day. For the emulsions with MUC32 :FA = 1 : 4% by weight,  $\tau_B$  increased with aging time until aging time was 14 days.  $\tau_B$  slightly decreased and became constant after 14 aging days.

#### 4.1.2 Optical Measurement

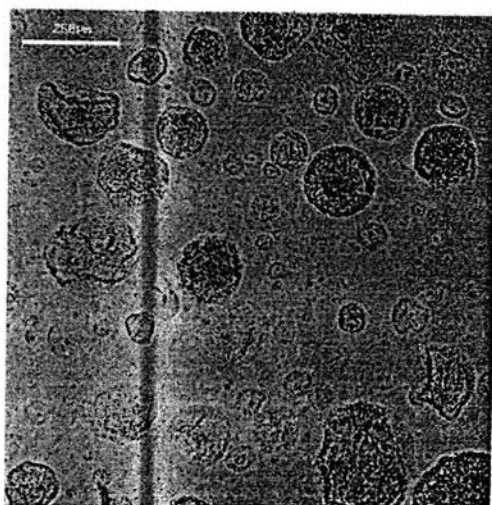
Figures 4.6 and 4.7 show micrographs of emulsions at various compositions of fatty alcohol as a function of aging time. Two different magnifications, 100 and 1000 were used in this experiment. For the emulsion with MUC32:FA = 1:2% by weight, very small size of dispersed particle can be seen under the 100 magnification micrograph of Figure 4.6a. These particles became slightly larger as the system aged (Figure 4.6b). The detailed structure can be seen under the 1000 magnification micrographs in Figure 4.7a and 4.7b. The micrographs show thin oriented multilayers of lamellar structures even as the system aged. The amount of fatty alcohol present in the system were not enough to interact with surfactant to form prominent lamellar structures. For the emulsions with MUC32:FA = 1:6 and 1:8 % by weight, various sizes of dispersed particles can be seen under the 100 magnification micrographs in the Figure 4.6 e, f, g and h. The sizes of the particles did not change significantly with aging time. Densely packed dark sheet lamellar layers or islands can be seen under the 1000 magnification micrographs due to the excess amount of fatty alcohol present in the system. For the emulsion with MUC32:FA = 1:4% by weight, nearly the same sizes of particles can be seen at aging time of 1 day under the 100 magnification micrographs of Figure 4.6c. These particles became larger when the system aged (Figure 4.6d). Thus viscosity of emulsion increased when dispersed particles of emulsion aggregated. Initially, surfactant and fatty alcohol interacted to form a lamellar structure. Later, the unreacted surfactant penetrated slowly into the crystalline alcohol to form additional network structures. Therefore, its viscosity increased as the system aged. Randomly oriented multilayer lamellar structure can be observed under the 100 magnification micrographs (Figure 4.7). The interlamellar spacings were fairly uniform after the aging time of 1 day. When system reached its equilibrium, which was around 14 days, dark sheet of fatty alcohol can be seen between some layers of the lamellar structures.



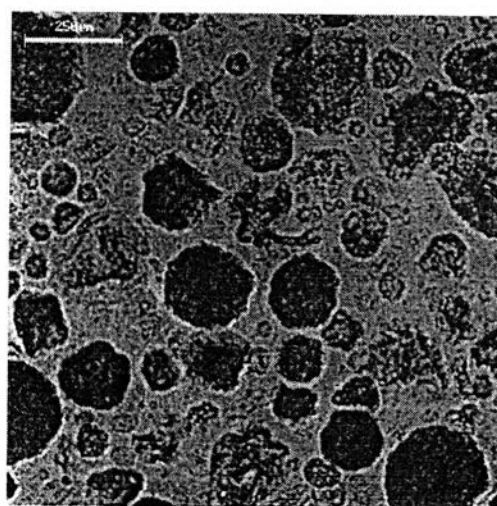
(a)



(b)



(c)



(d)

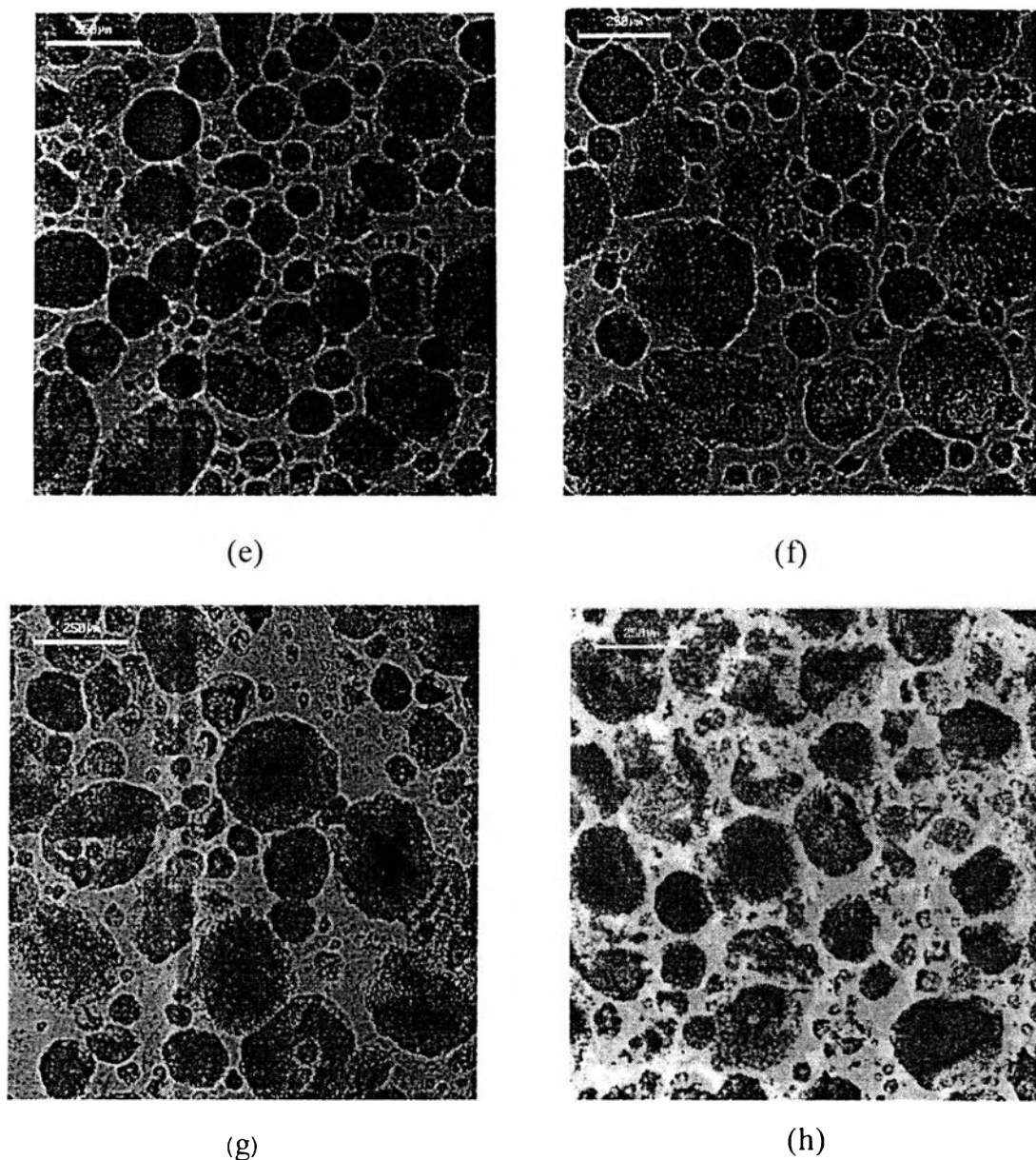


**Figure 4.6** Micrographs of emulsion obtained at 100 magnification as a function of aging time: (a) MUC32:FA = 1:2 at 1day; (b) MUC32:FA = 1:2 at equilibrium; (c) MUC32:FA = 1:4 at 1day; (d) MUC32:FA = 1:4 at equilibrium ; (e) MUC32:FA = 1:6 at 1day; (f) MUC32:FA = 1:6 at equilibrium; (g) MUC32:FA = 1:8 at 1 day ; (h) MUC32:FA=1:8 at equilibrium, temperature was equal to  $26 \pm 1^{\circ}\text{C}$ , and pH was between 8.7-9.2.

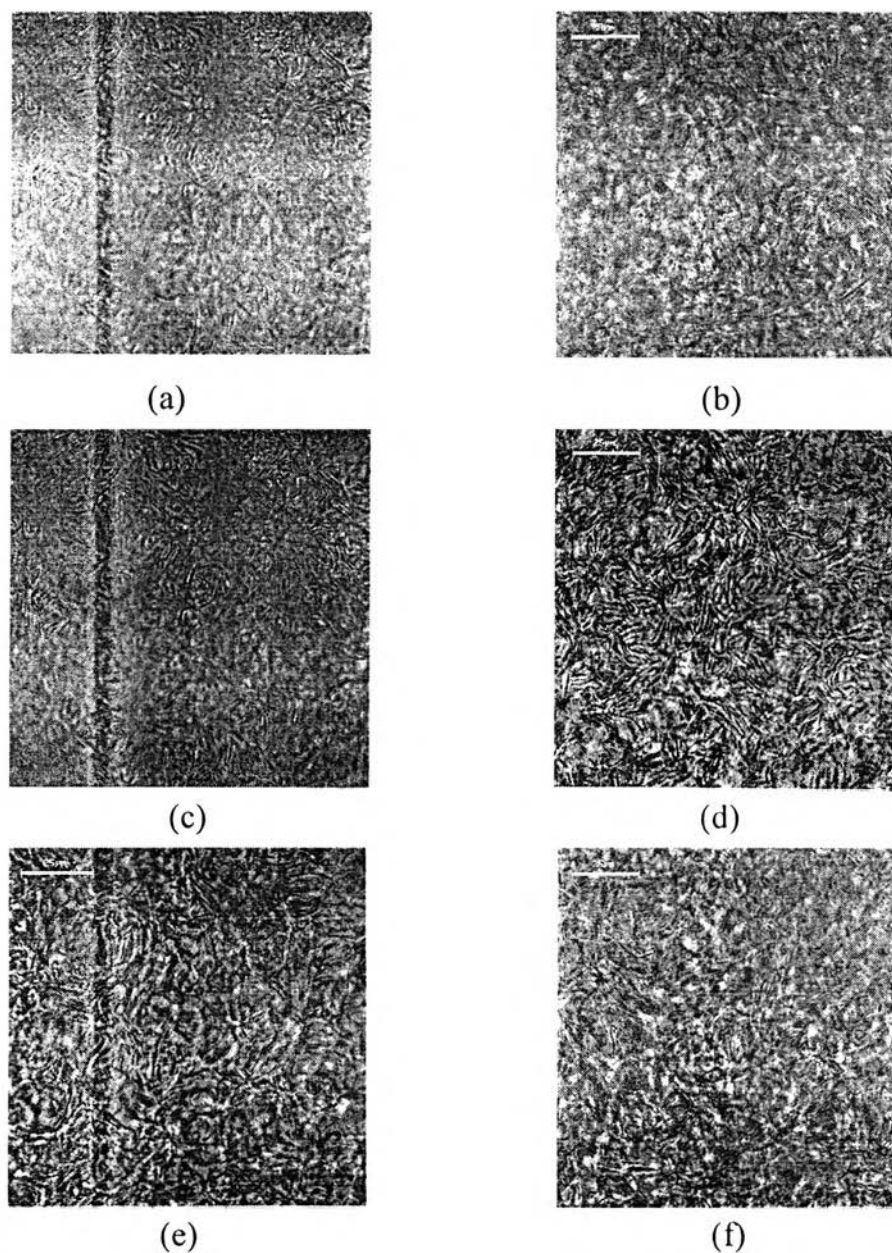


**Figure 4.7** Micrographs of emulsions obtained at 1000 magnification as a function of aging time: (a) MUC32:FA = 1:2 at 1 day; (b) MUC32:FA = 1:2 at equilibrium; (c) MUC32:FA = 1:4 at 1 day; (d) MUC32:FA=1:4 at equilibrium; (e) MUC32:FA = 1:8 at 1 day; (f) MUC32:FA=1:8, temperature was equal to  $26\pm 1^{\circ}\text{C}$ , and pH was 8.7-9.2.

## 4.2 Effect of Fatty Alcohol Concentrations on Emulsion Structure

### 4.2.1 Rheological Measurement

#### 4.2.1.1 Zero Shear Viscosity

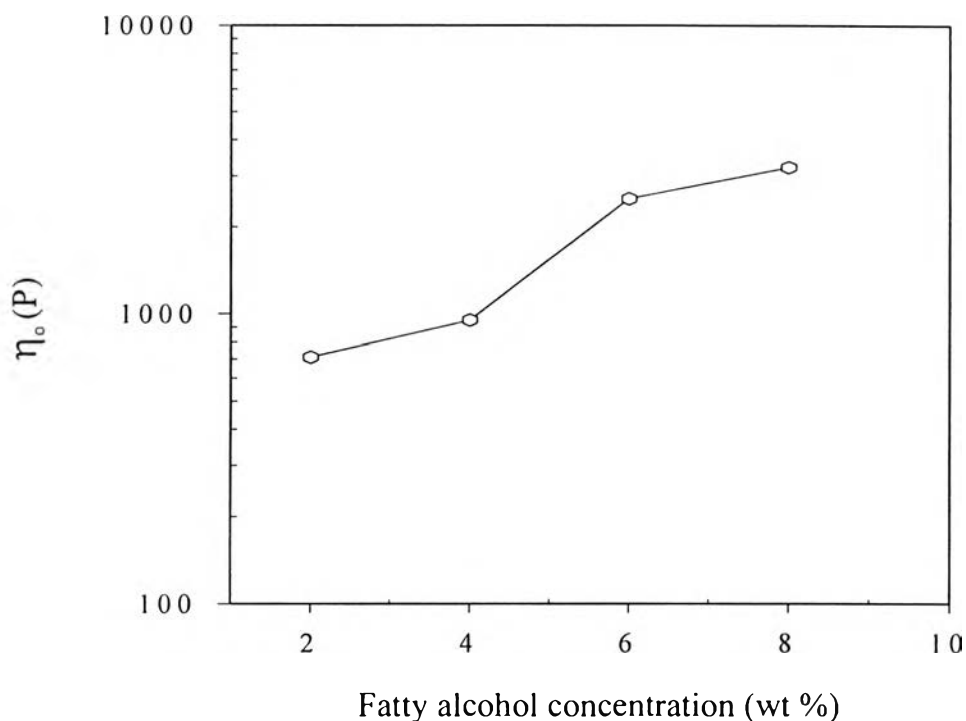


**Figure 4.8** Zero shear viscosity ( $\eta_0$ ) against fatty alcohol concentration of various emulsions;  $\eta_0$  was  $\eta$  at shear rate  $0.01 \text{ s}^{-1}$ , temperature was  $26 \pm 1^\circ\text{C}$ , and pH was between 8.7-9.2.

Figure 4.8 shows the zero shear viscosity versus fatty alcohol concentration. Zero shear viscosity increased as fatty alcohol concentration was varied from 2, 4 and 6% by weight. As fatty alcohol increased from 6 to 8% by weight, the zero shear viscosity became constant. The data suggest that the saturation level of fatty alcohol concentration was obtained at 6 to 8% by weight, as excess fatty alcohol concentration were present in the emulsions with MUC32:FA = 1:6 and 1:8% by weight. Our

results are consistent with those of Talman *et al.* (1987) who found that the rheology can be controlled by adding the cetostearyl alcohol.

#### 4.2.1.2 Entanglement Storage Modulus

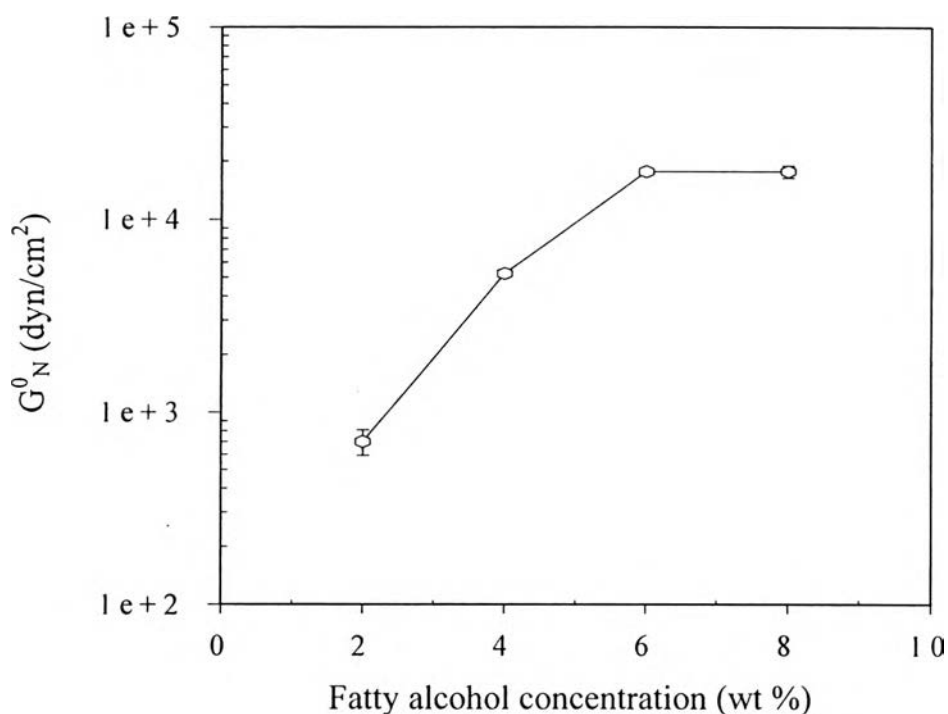


**Figure 4.9** Entanglement storage modulus ( $G_N^0$ ) against fatty alcohol concentration;  $G_N^0$  was  $G'(\omega)$  at 100 rad/s, temperature was  $26 \pm 1^\circ\text{C}$ , strain was 0.2%, and pH was between 8.7-9.2.

Figure 4.9 shows the value of  $G_N^0$  against fatty alcohol concentration. The value of  $G_N^0$  increased from  $1.0 \times 10^3$  to  $2.0 \times 10^4$  dyn/cm<sup>2</sup> and reached a saturation level as fatty alcohol content was varied from 2 to 8 % by weight. The data suggest that the emulsions with more fatty alcohol content were relatively more elastic.



#### 4.2.1.3 Bingham Stress

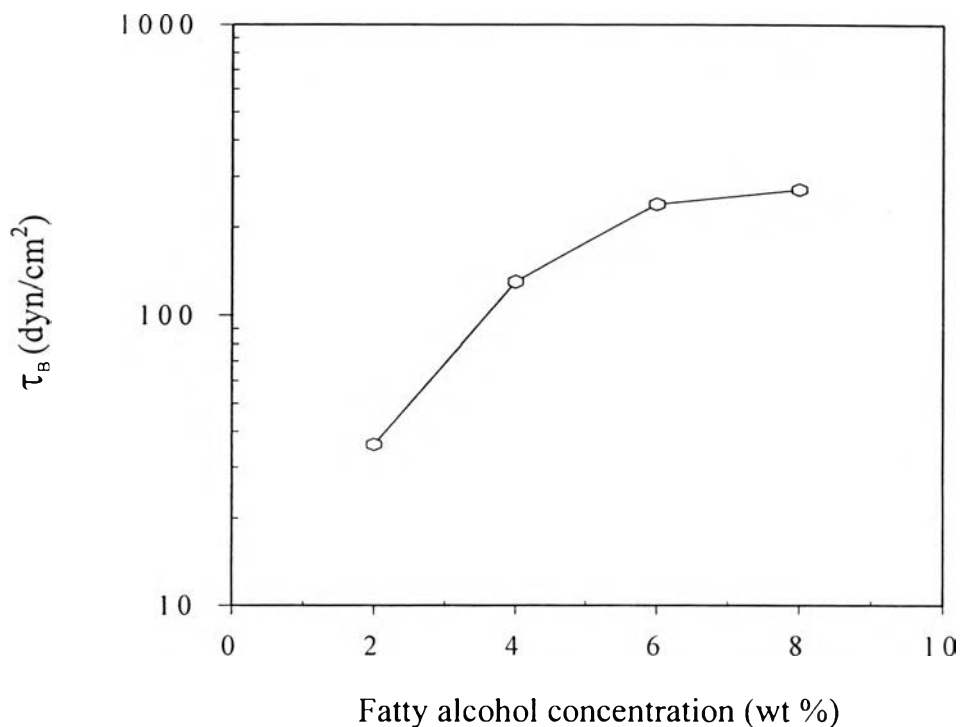


**Figure 4.10** Bingham stress ( $\tau_B$ ) against fatty alcohol concentration of various emulsions; temperature was  $26 \pm 1^\circ\text{C}$ , and pH was between 8.7-9.2.

Figure 4.10 shows the yield stress versus fatty alcohol concentration. This plot shows the same behavior as the entanglement storage modulus. The higher zero shear rate viscosity, the higher stress or force was required to initiate the flow of emulsion.

#### 4.2.2 Optical Measurement

Figures 4.11 and 4.12 show the micrographs of the emulsions with various fatty alcohol concentrations at two different magnifications: 100 and 1000 using the laser scan microscope. There was a growth of dispersed particle with increasing fatty alcohol concentration 2, 4 and 6% by weight as can be seen in the 100 magnification micrographs of Figure 4.11. As fatty alcohol composition was increased from 6 to 8% by weight, the system became very condensed and sizes did not change significantly with fatty alcohol concentration (Figures 4.11c and 4.11d). The detail structure of the every system can be observed in 1000 magnification micrographs of Figure 4.12.

The 100 magnification micrographs (Figure 4.11) show dispersed particles of various sizes at various fatty alcohol contents. The size of dispersed particles became significantly larger with fatty alcohol concentrations.

The 1000 magnification micrographs (Figure 4.12) show thin randomly oriented multilayers of lamellar structures at the fatty alcohol composition of 2% by weight. When fatty alcohol was varied from 2 to 4% by weight, these thin lines were more pronounced and additional network structure appear (Figure 4.12a and 4.12b). At fatty alcohol composition of 2% by weight, there was not enough fatty alcohol to interact with all surfactant molecules present in the system. Therefore some of the excess of surfactant were left in the system. However, surfactant aggregates alone cannot be seen under the microscope. At high fatty alcohol concentrations of 6 and 8% by weight, densely packed dark sheet multilayers lamellar structures were formed in the system. Sometimes it remained as islands between the lamellar layers. This implies that the amount of surfactant was not enough to interact with all fatty alcohol molecules present in the system. Therefore, some excess amount of fatty alcohol remained in the system (Figure 4.12c and 4.12d).

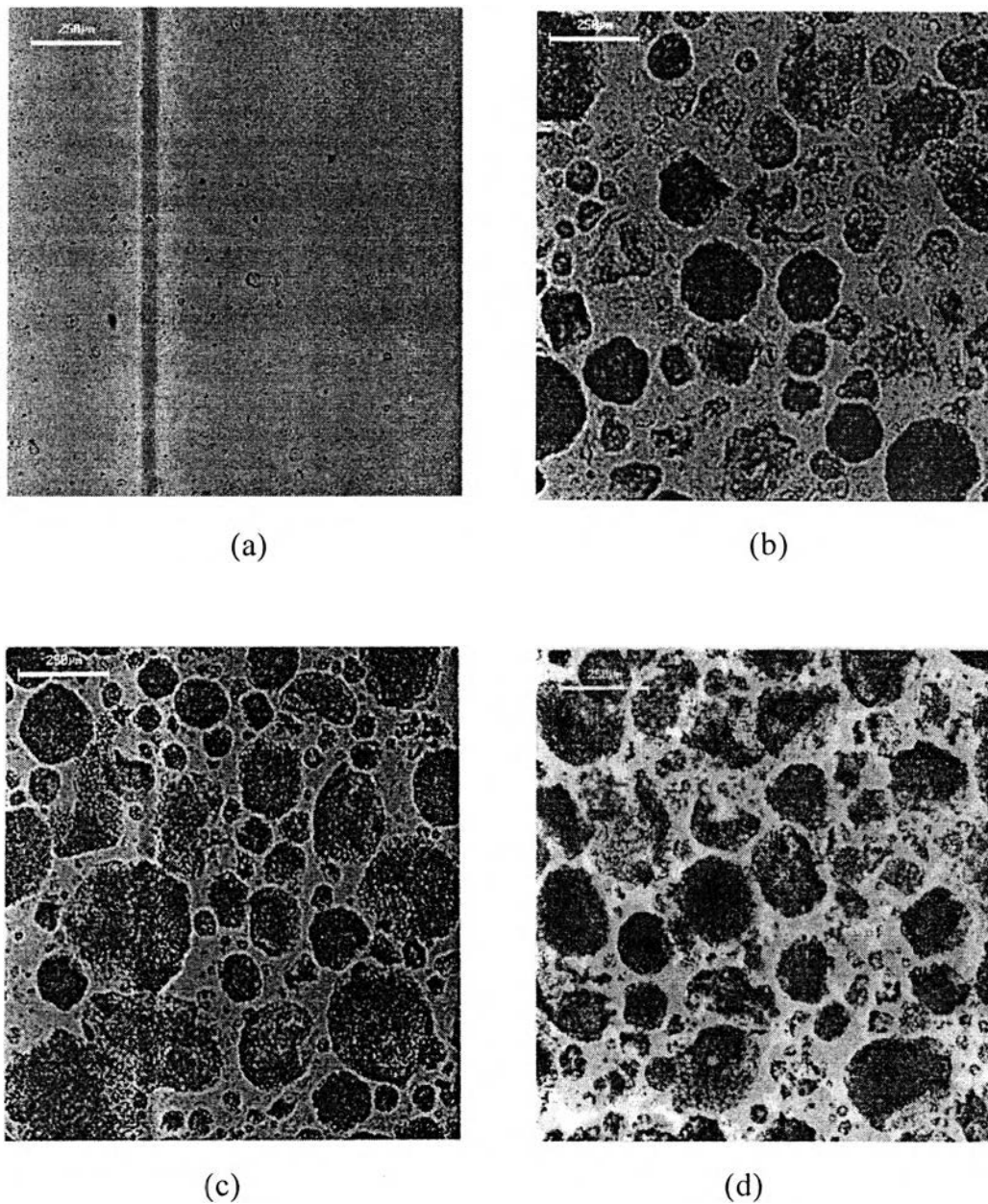


**Figure 4.11** Micrographs of emulsion obtained at 100 magnification as a function of fatty alcohol concentration: MUC32:FA = 1:2; (b) MUC32:FA=1:4; (c) MUC32:FA=1:6; (d) MUC32:FA=1:8% by weight, temperature was equal to  $26 \pm 1^{\circ}\text{C}$ , and pH was between 8.7-9.2.

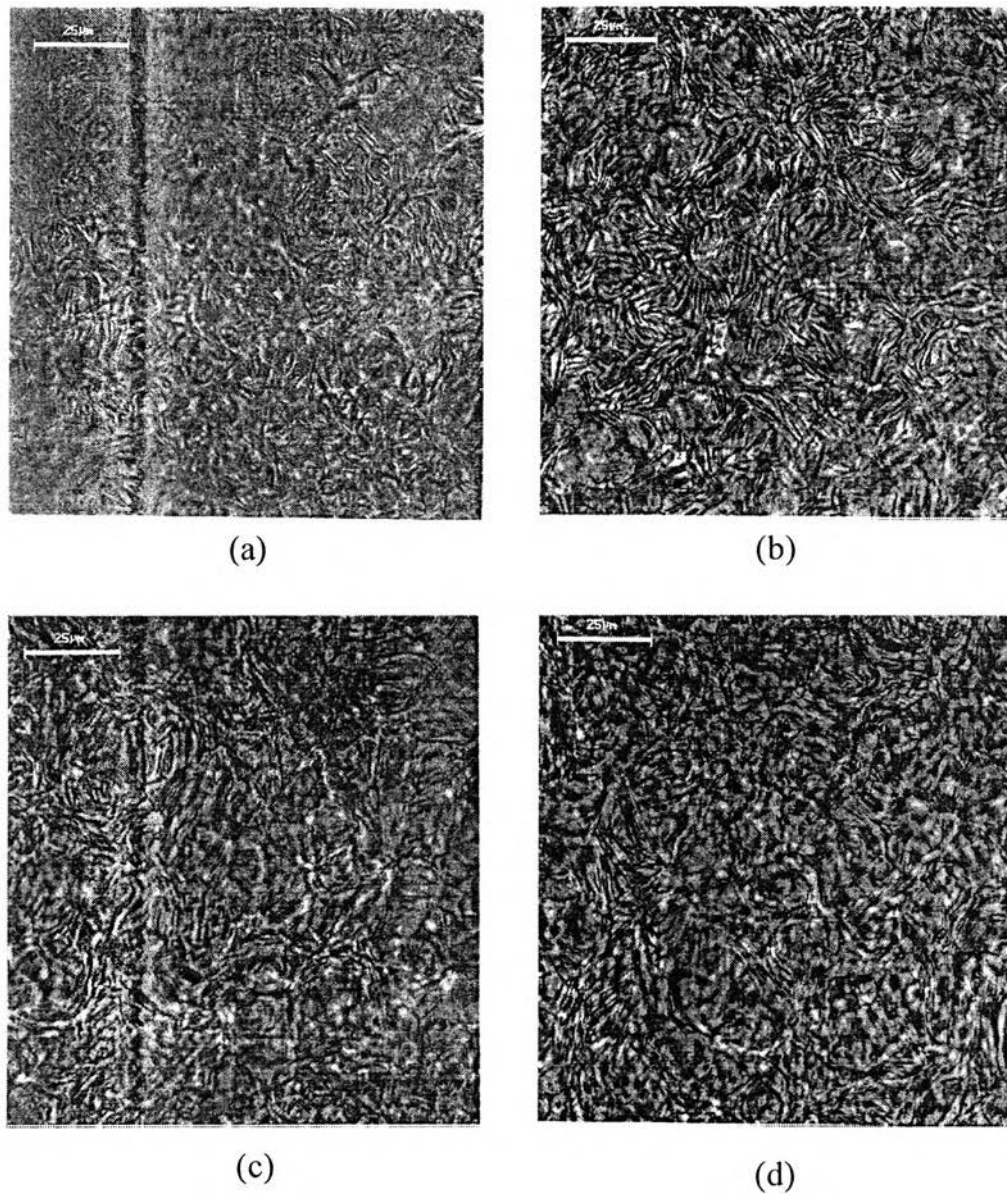
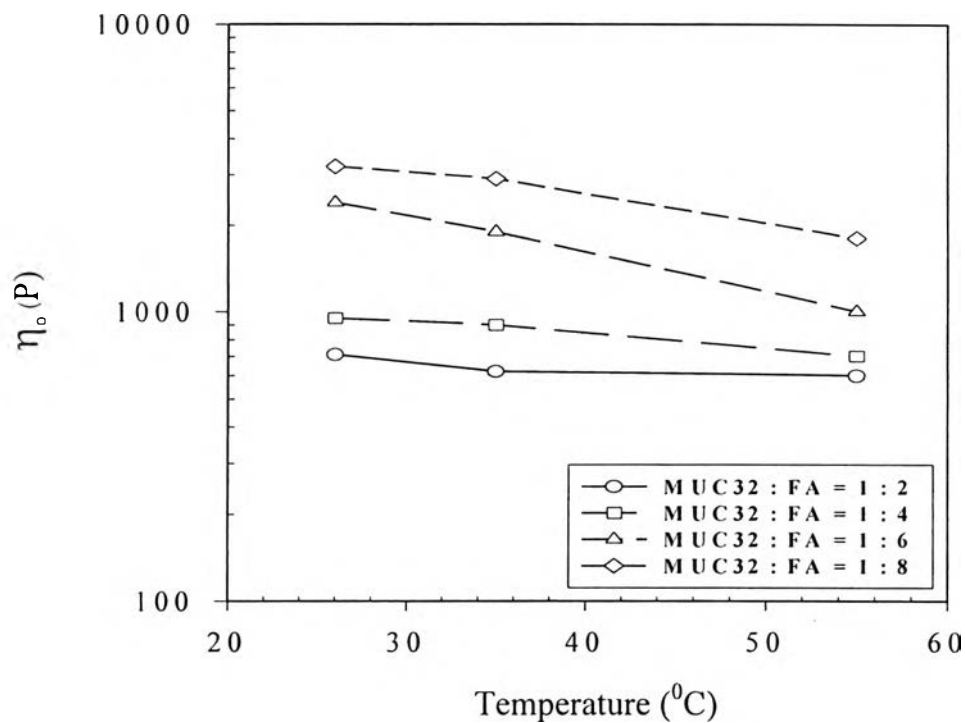


**Figure 4.12** Micrographs of emulsion obtained at 1000 magnification as a function of fatty alcohol concentration: (a) MUC32:FA = 1:2; (b) MUC32:FA = 1:4; (c) MUC32:FA = 1:6; (d) MUC32:FA=1:8% by weight, temperature was equal to  $26\pm 1^{\circ}\text{C}$ , and pH was between 8.7-9.2.

### 4.3 Effect of Temperature on Emulsion Structure

#### 4.3.1 Rheological Measurement

##### 4.3.1.1 Zero Shear Viscosity



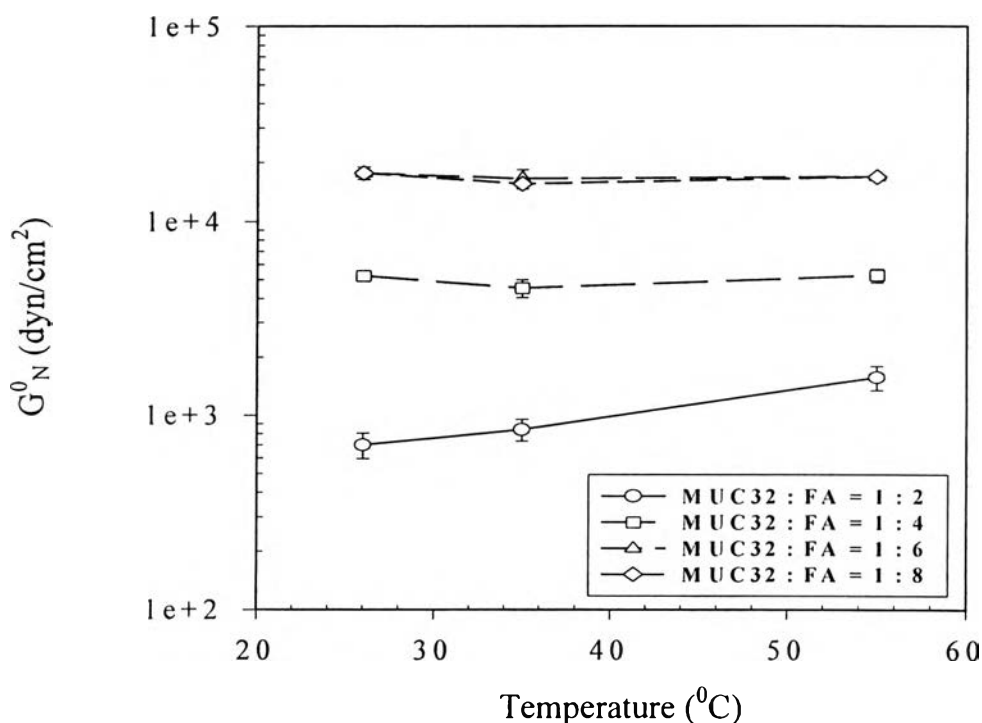
**Figure 4.13** Zero shear viscosity ( $\eta_0$ ) against temperature of various emulsions;  $\eta_0$  was  $\eta$  at shear rate of  $0.01 \text{ s}^{-1}$ , temperatures were 26, 35, 55°C, and pH was between 8.7-9.2.

Figure 4.13 shows the zero shear viscosity versus temperature. The zero shear viscosity decreased with increasing temperature especially at higher ratios of fatty alcohol concentration. The data suggest that the samples behaved as Newtonian liquids. The viscosity of Newtonian liquid decreases with temperature according to the Arrhenius relationship (Hunter, 1993):

$$\eta = A e^{B/T} \quad (\text{Eq. 4.1})$$

where  $T$  is the absolute temperature and  $A$  and  $B$  are constants of the liquid. In general, for Newtonian liquids, the greater the viscosity, the stronger is the temperature dependence. Therefore, the higher amount of fatty alcohol ratio shows the greater temperature dependence.

#### 4.3.1.2 Entanglement Storage Modulus



**Figure 4.14** Entanglement storage modulus ( $G_N^0$ ) against temperature;  $G_N^0$  was  $G'$  at 100 rad/s, temperatures were 26, 35, 55°C, strain was 0.2%, and pH was in the range of 8.7- 9.2.

For the emulsions with surfactant and fatty alcohol ratios of 1 to 4, 6 and 8% by weight,  $G_N^0$  were nearly constant with temperature. This can be explained by a transient junction in the network (Larson, 1999). At any instant, junctions were fairly permanent for the network to behave like a rubber but they broke after a short lifetime and reformed elsewhere, hence the system

was capable of flowing. Since the total concentration of junctions always remained constant, therefore elastic properties were constant. Balzer *et al.* (1996) found that the temperature had no influence upon the network structure, but had a strong effect on viscosity and the yield stress.

#### 4.3.1.3 Bingham Stress

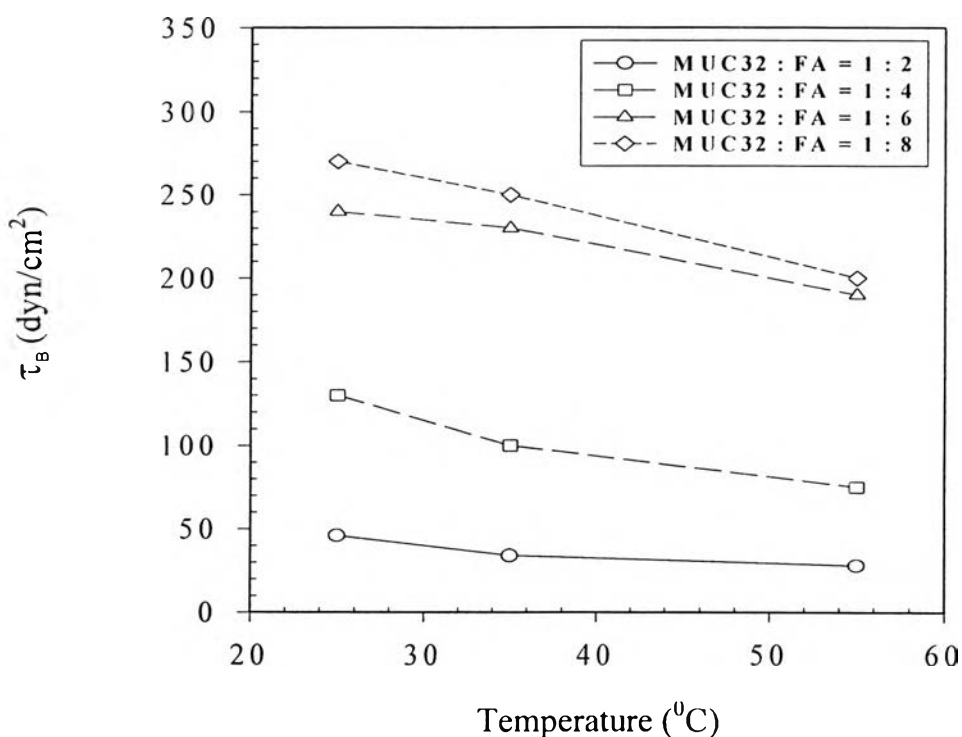


**Figure 4.15** Bingham stress ( $\tau_B$ ) against temperature of various emulsions; temperatures were 26, 35, 55 $^{\circ}\text{C}$ , and pH was between 8.7-9.2.

Figure 4.15 shows the yield stress versus temperature. It shows the same behavior as the zero shear viscosity. Force or stress required to initiate the flow decreased with temperature. The higher the viscosity the greater the percent change occurred. The stress was slightly changed at low fatty alcohol concentration.

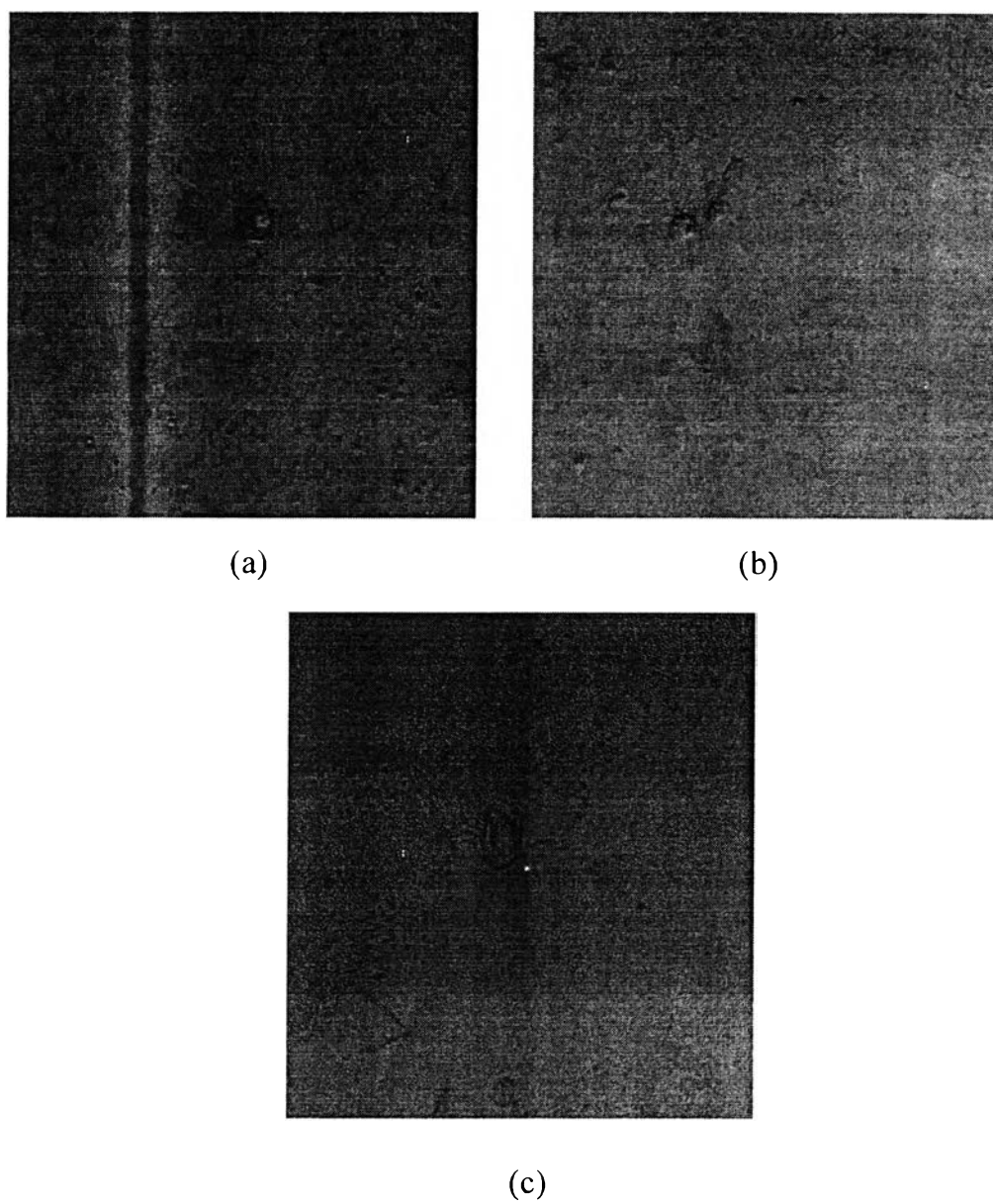
### 4.3.2 Optical Measurement

Figure 4.16 to 4.18 show the micrographs of the emulsion with MUC32:FA = 1:2, 1:4, and 1:8% by weight.

For the emulsions with MUC32:FA=1:4 and 1:8% by weight (Figure 4.17 and 4.18), when temperature was raised from 26 to 35<sup>0</sup>C, there was no significant change. The melting point of the fatty alcohol is 48-53<sup>0</sup>C. When temperature was raised from 35 to 55<sup>0</sup>C, which is above the melting point of fatty alcohol, the dispersed particles aggregates disaggregated and size became smaller. Also the amount of dispersed particles increased with temperature. At that temperature, the excess of fatty alcohol crystalline present in the system was melted when temperature was increased above the melting point of fatty alcohol. Therefore the larger size of dispersed particles aggregates disaggregated and dispersed into the matrix.

For the emulsion with MUC32:FA=1:2% by weight, the micrograph does not show a significant change at the three temperatures. This was because excess fatty alcohol crystalline did not exist in the system and the sizes of the dispersed particles were very small to see the effect under the optical microscope.





**Figure 4.16** Micrographs of emulsion obtained at 1000 magnification of MUC32:FA = 1:2% by weight as a function of temperature: (a) 26<sup>0</sup>C; (b) 35<sup>0</sup>C; (c) 55<sup>0</sup>C, and pH was between 8.7-9.2.

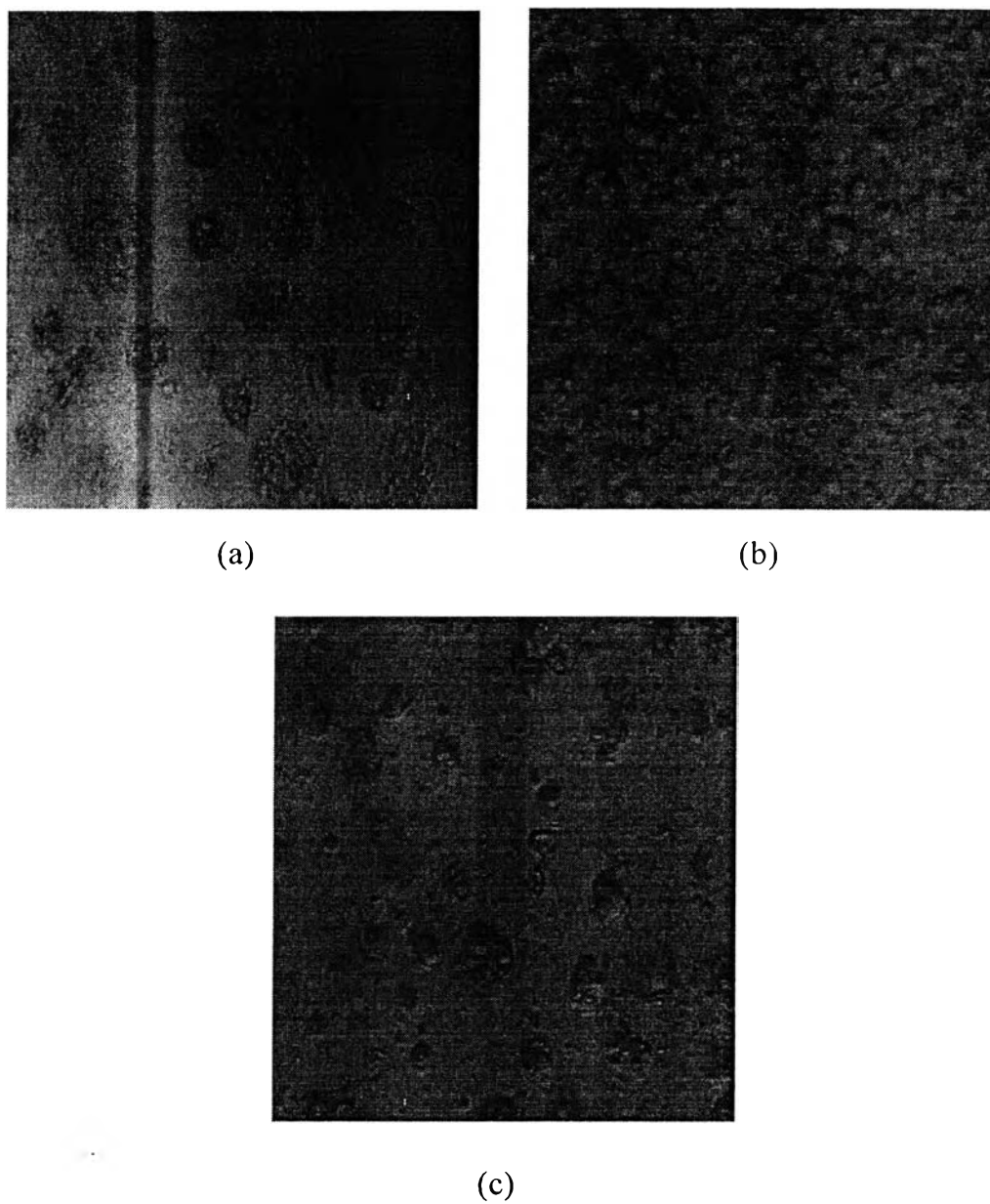


**Figure 4.17** Micrographs of emulsion obtained at 1000 magnification of MUC32:FA = 1:4% by weight as a function of temperature: (a) 26<sup>0</sup>C; (b) 35<sup>0</sup>C; (c) 55<sup>0</sup>C, and pH was between 8.7-9.2.

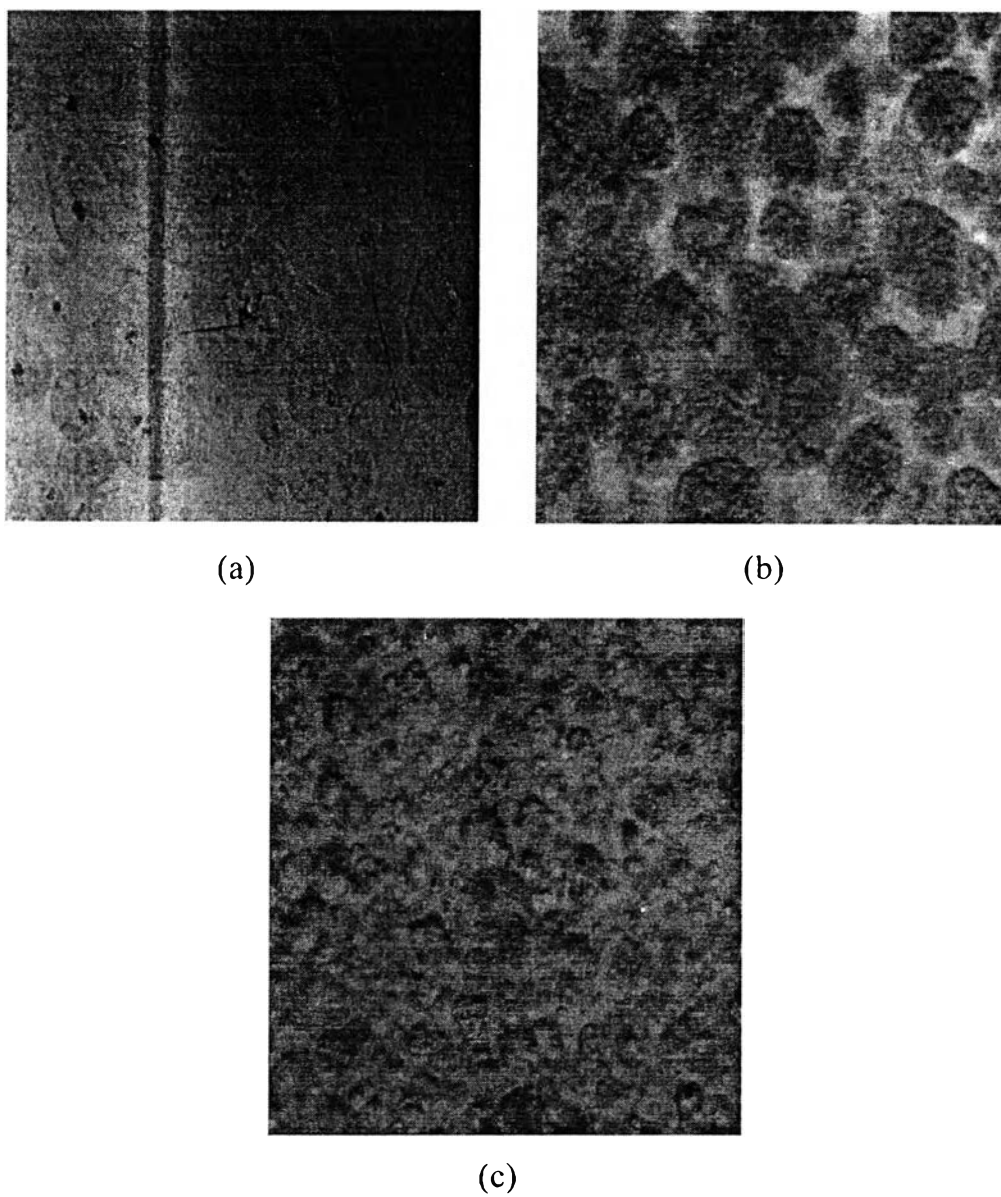


**Figure 4.18** Micrographs of emulsion obtained at 1000 magnification of MUC32:FA = 1:8% by weight as a function of temperature: (a) 26<sup>0</sup>C; (b) 35<sup>0</sup>C; (c) 55<sup>0</sup>C, and pH was between 8.7-9.2.

## 4.4 Effect of pH on Emulsion Structure

### 4.4.1 Characterization of Surfactant

#### 4.4.1.1 *Zeta-Potential Measurement*

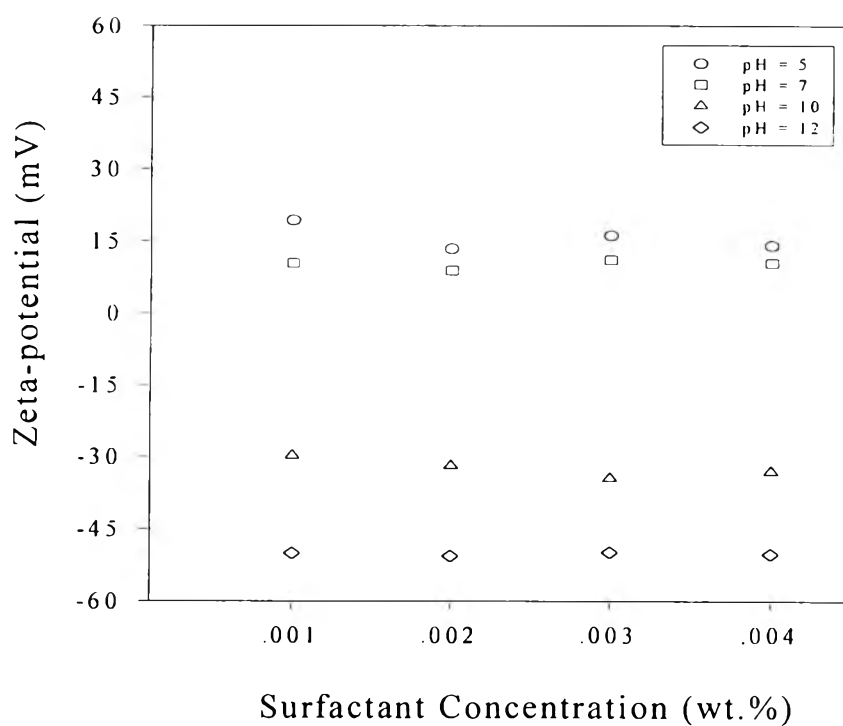


**Figure 4.19a** Zeta-potential against surfactant concentration; temperature was equal to  $26 \pm 1^{\circ}\text{C}$ .

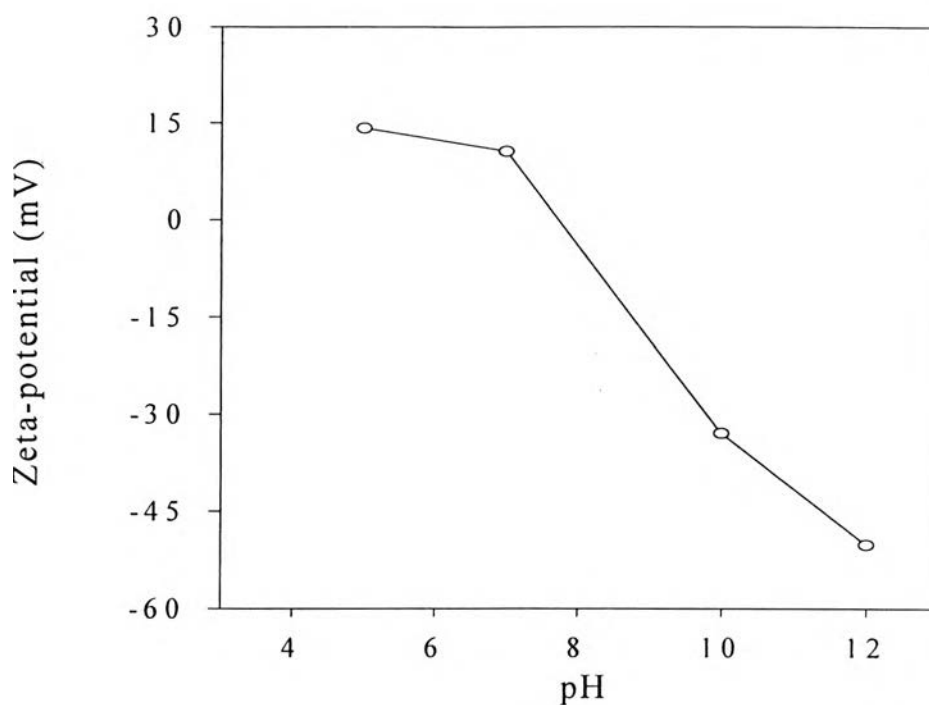


**Figure 4.19b** Zeta-potential against pH; temperature was equal to  $26 \pm 1^{\circ}\text{C}$ .

Figure 4.19a and 4.19b show the zeta-potential measurement of surfactant. Surfactant solutions at high pH values, pH 10 and pH 12 showed the anionic behavior. At low pH values, pH 5 and pH 7, surfactant solutions possessed the cationic behavior. Isoelectric point of the surfactant solution was in the range of pH between 8 to 9.

#### 4.4.2 Rheological Measurement

##### 4.4.2.1 Zero Shear Viscosity

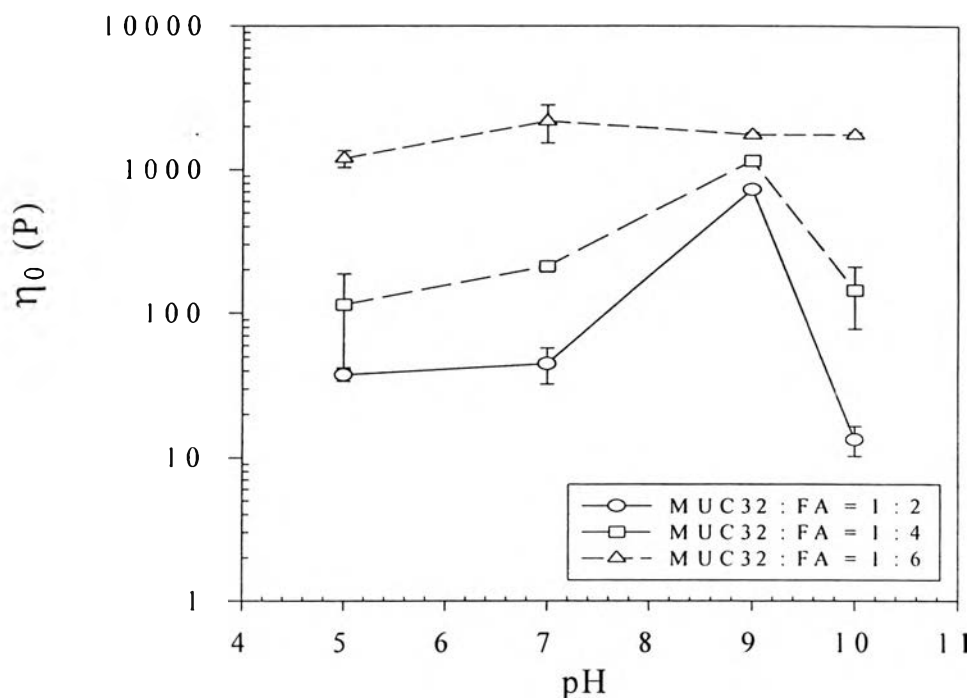


**Figure 4.20** Zero shear viscosity ( $\eta_0$ ) against pH; temperature was equal to  $26 \pm 1^\circ\text{C}$ , and pH were 5, 7, 8.7-9.2 and 10.

Figure 4.20 shows the zero shear viscosity against pH at the temperature of  $26^\circ\text{C}$ . The data give the highest value at pH around 8.7 – 9.2, which was the isoelectric point of the surfactant. At the isoelectric area, the head group or hydrophilic part of the surfactant possessed both positive charges and negative charges with roughly equal number. At that condition, surfactant molecules could easily interact with a fatty alcohol to form a network structure or lamellar phase due to hydrophilic attraction. Hence, the zero viscosity was highest at the point.

Outside region of the isoelectric point, such as pH 5, 7 or 10 the zero shear viscosity decreased. Below the isoelectric region, the hydrophilic part of the surfactant molecules consisted of more positive charges

whereas above the isoelectric point it consisted of more negative charges. Thus viscosity decreases due to hydrophilic repulsion.

pH had no influence on the high fatty alcohol concentration emulsion due to the excess of fatty alcohol amount present in the system.

#### 4.4.2.2 Entanglement Storage Modulus

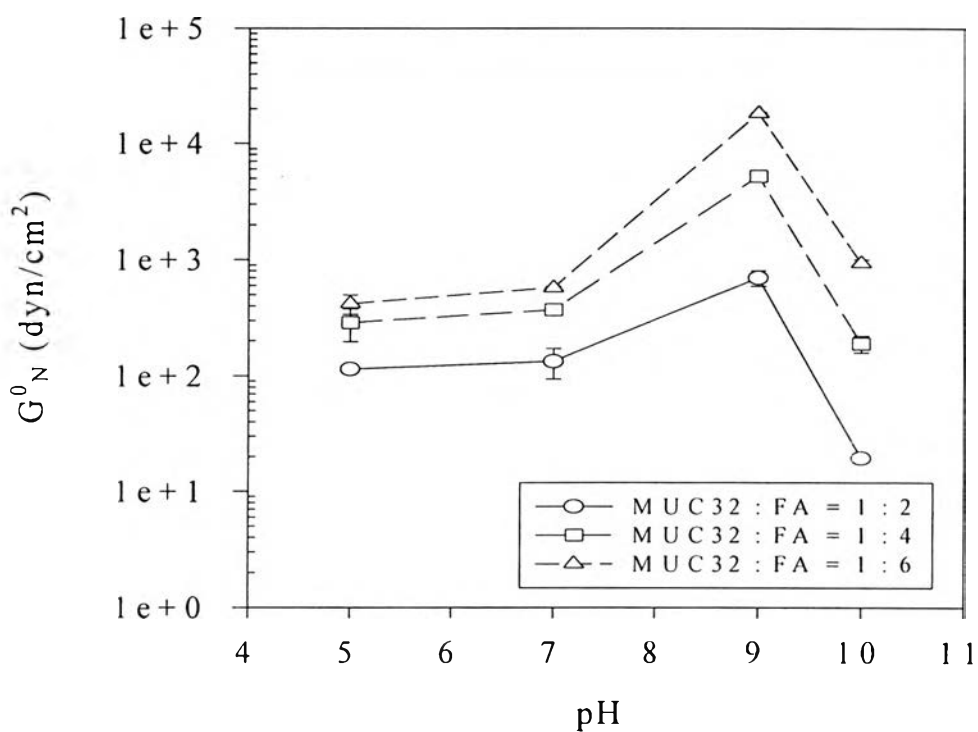


**Figure 4.21** Entanglement storage modulus ( $G_N^0$ ) against pH; temperature was equal to  $26 \pm 1^\circ\text{C}$ , and pH were 5, 7, 8.7-9.2 and 10.

Figure 4.21 shows the entanglement storage modulus against pH. The graph shows the same behavior as the zero shear viscosity. However, at high concentration of fatty alcohol, entanglement storage modulus changed with pH. The network structure was disturbed when HCl or  $\text{NH}_4\text{OH}$  was added to the emulsion in order to adjust the pH. Therefore, the entanglement modulus decreased with increasing or and decreasing pH. Thus, the system had a low entanglement modulus with high viscosity.

#### 4.4.2.3 Bingham Stress

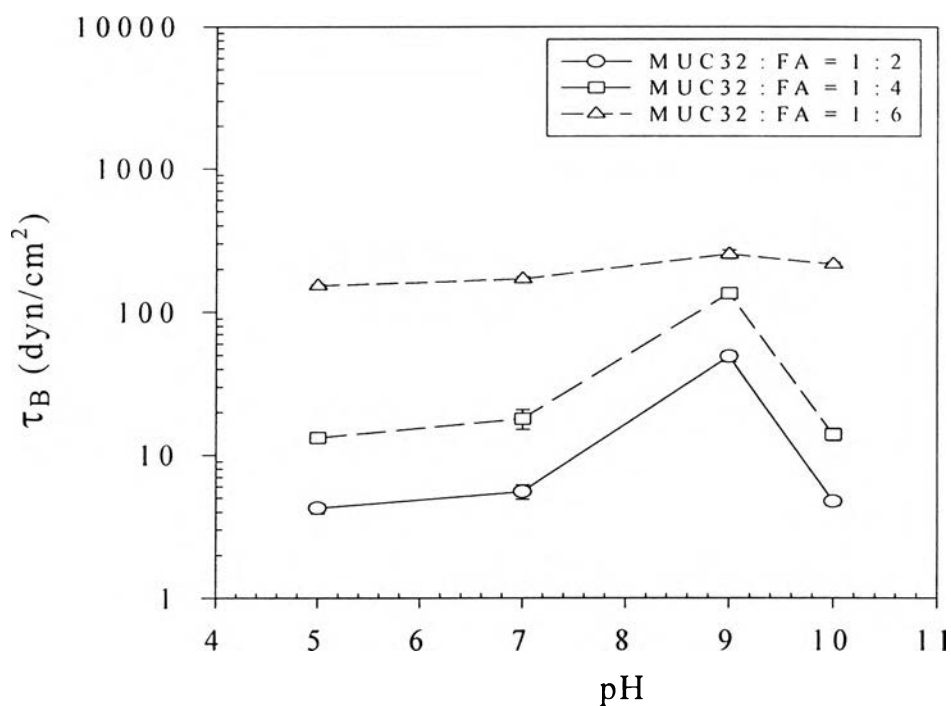


**Figure 4.22**  $\tau_B$  against pH; temperature was equal to  $26 \pm 1^\circ\text{C}$ , and pH were 5, 7, 8.7-9.2.

Figure 4.22 shows the Bingham stress against pH. The graph shows the same behavior as the zero shear viscosity. The higher the viscosity the more force was required to initiate the flow. Thus, isoelectric area had the highest value of Bingham stress than those of low and or high pH.



#### 4.4.3 Optical Measurement

Figures 4.24 to 4.29 show the micrographs of the emulsion with various compositions of fatty alcohol at varying pH. The micrographs were taken under 100 and 1000 magnifications respectively. The morphology significantly changed with pH as can be seen at both magnifications.

The 100 magnification micrographs, of Figure 4.24 and 4.25 for the emulsions with MUC32:FA=1:2 % and 1:4% by weight, indicate different morphology with varying pH. Spherical droplets can be seen to be far apart from each other when pH was about the isoelectric regime due to hydrophilic repulsion of the surfactant molecules. The hydrophilic part of surfactant molecule of the emulsion at pH 5 had more positive charges than the emulsion at pH 7. Therefore, hydrophilic repulsion was more pronounced at value of pH 5. Thus viscosity was slightly lower in the emulsion with pH 5 than emulsion with pH 7. At the emulsion with pH 10, the hydrophilic part of surfactant molecule was dominant with negative charges. These charges not only repelled each other but also repelled the negatively charged fatty alcohol. Thus, the repulsion was greater. Hence, the viscosity was the lowest. The schematic drawing showing variation in ionic charge and closeness of packing for amphoteric surfactant at various pH as can be seen in Figure 4.23. For the emulsion of high fatty alcohol ratio of 6% by weight, no significant change in morphology due to the excess of fatty alcohol occurred; surfactant molecules were not enough to interact with fatty alcohol.

The detailed structure of the emulsion with surfactant and fatty alcohol can be seen under the 1000 magnification micrographs. Emulsions with surfactant and fatty alcohol ratio of 1 to 2% by weight formed the multilayer of lamellar structure at all pH. When the fatty alcohol composition was increased from 2 to 4% by weight, the dark sheet of the fatty alcohol layers can be seen between the multilayer lamellar structure. At high fatty

alcohol composition 6% by weight, we can observe multilamellar layers. These layers combined with dark sheet or islands of excess fatty alcohol. The lamellar layers were binding each other and form a bundle. Each bundle was surrounded by lamellar and which formed a boundary.

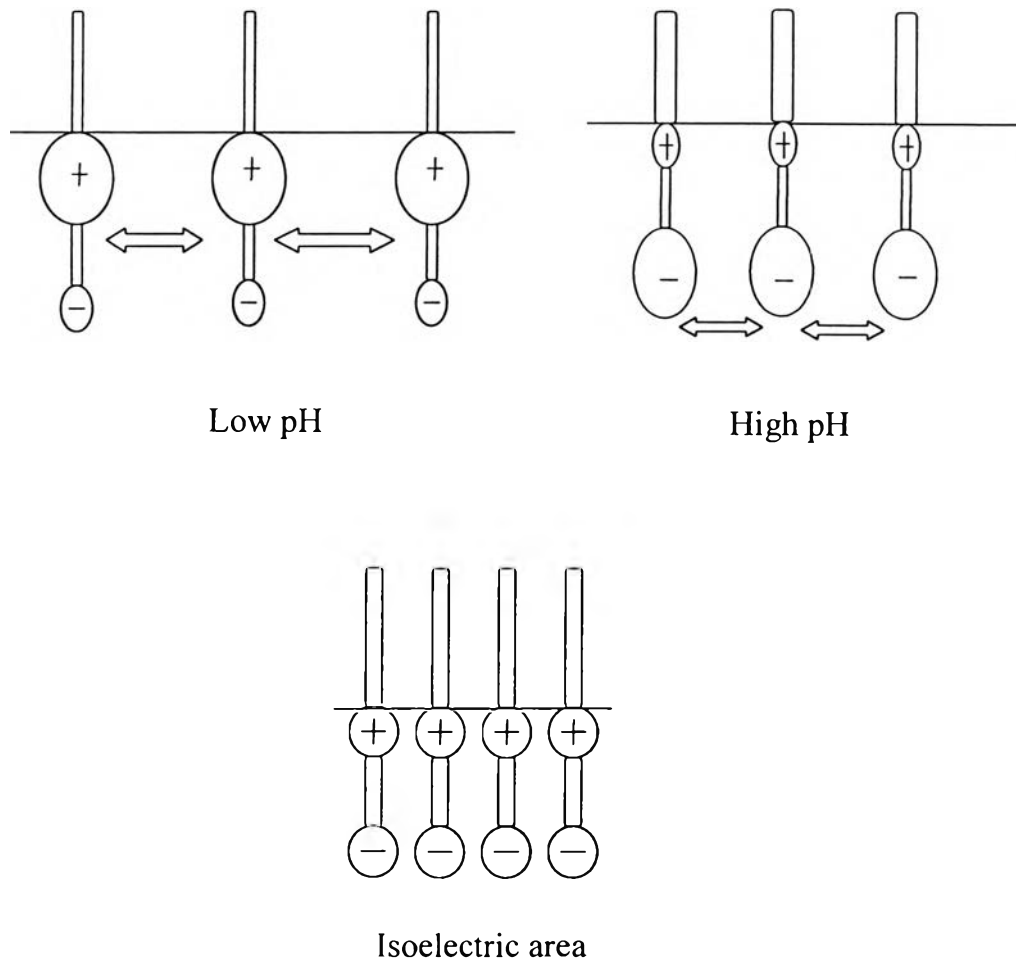


**Figure 4.23** Schematic drawing showing variation in ionic charge and closeness of packing for amphoteric surfactant at varying pH.

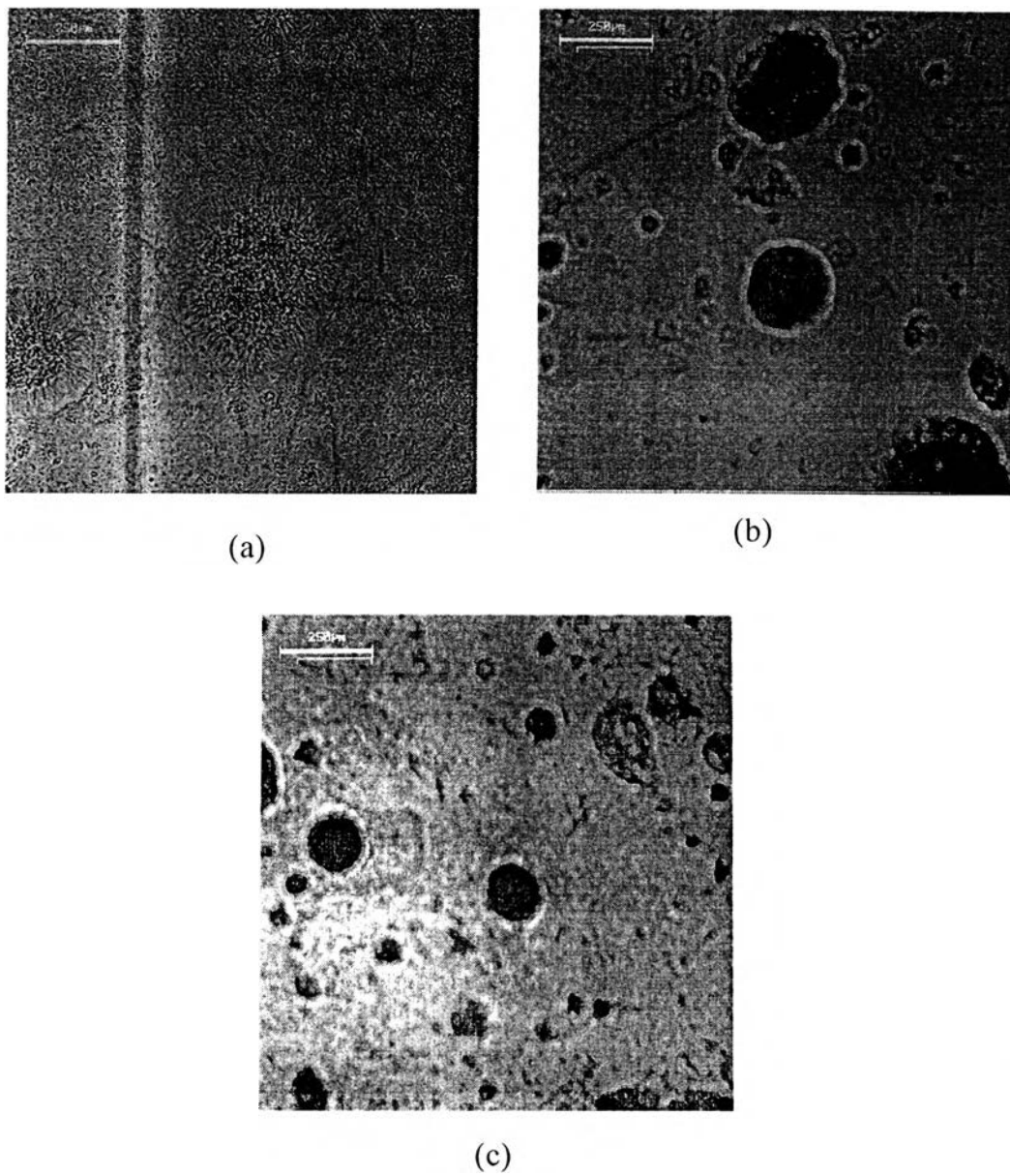


**Figure 4.24** Micrographs of emulsion obtained at 100 magnification of MUC32:FA=1:2% by weight as a function of pH: (a) pH = 5; (b) pH = 7; (c) pH = 10, and temperature was between  $26\pm 1^{\circ}\text{C}$ .

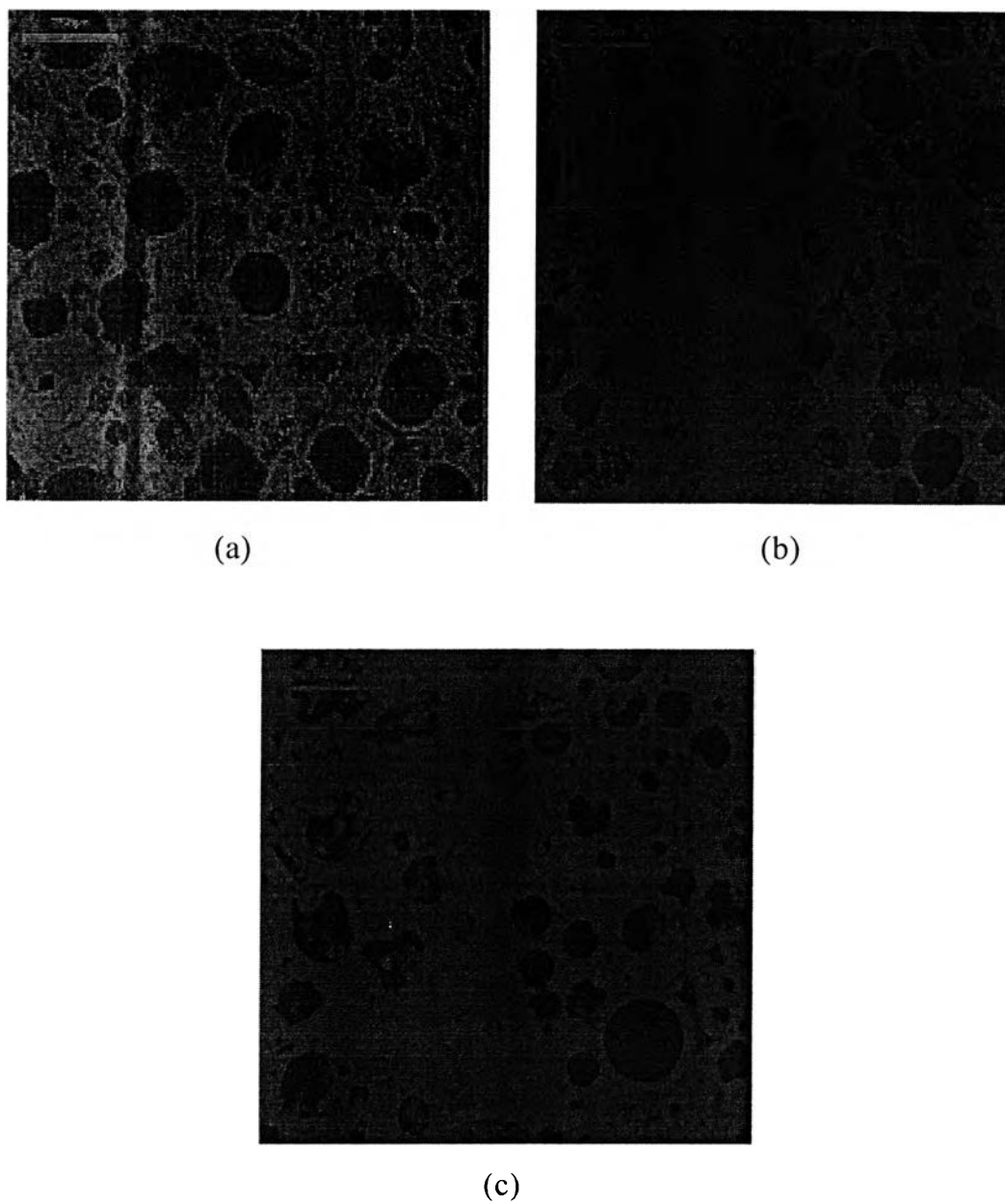


**Figure 4.25** Micrographs of emulsion obtained at 100 magnification of MUC32:FA=1:4% by weight as a function of pH: (a) pH = 5; (b) pH = 7; (c) pH = 10, and temperature was equal to  $26\pm 1^{\circ}\text{C}$ .

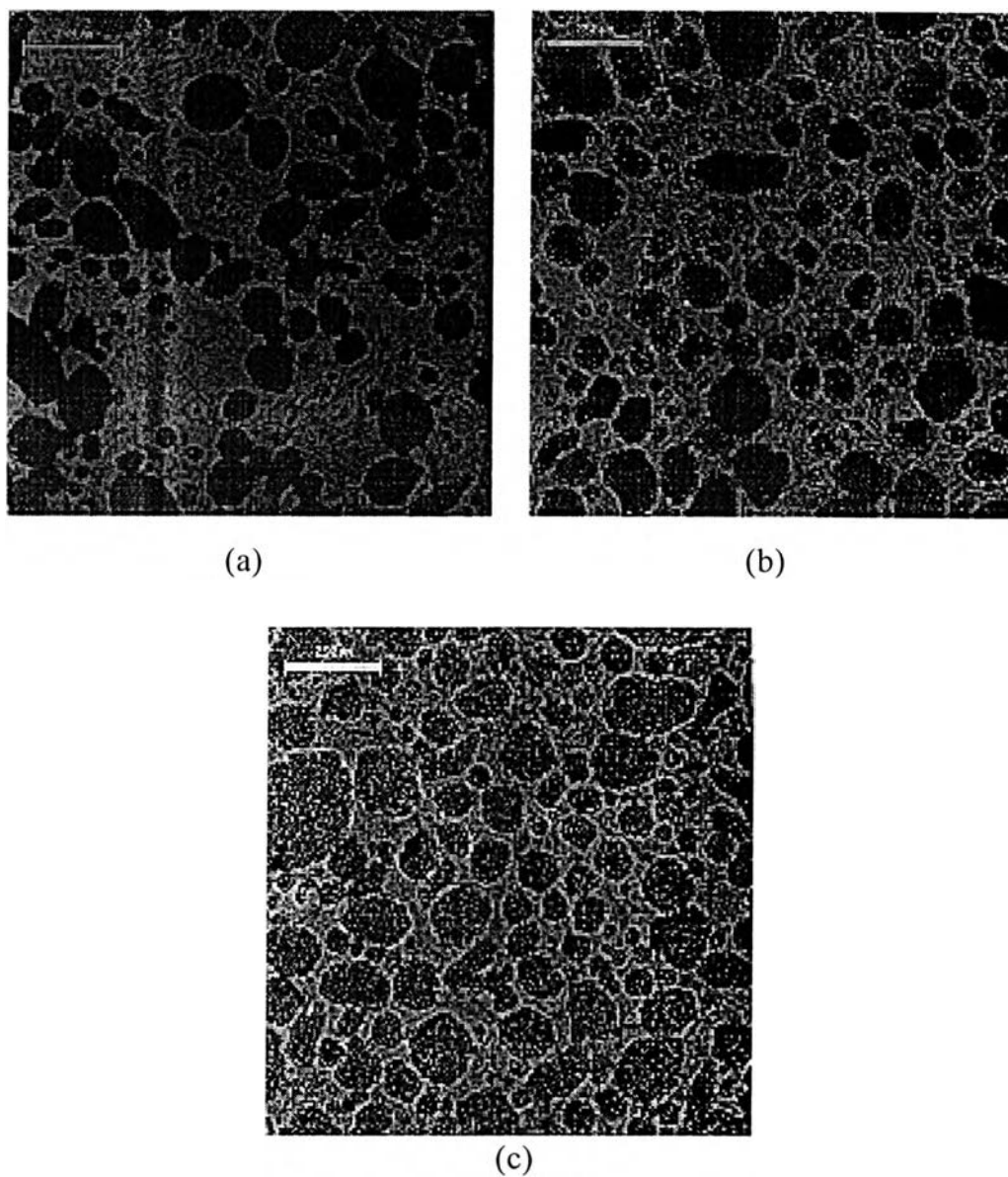


**Figure 4.26** Micrographs of emulsion obtained at 100 magnification of MUC32:FA=1:6% by weight as a function of pH: (a) pH = 5; (b) pH = 7; (c) pH = 10, temperature was between  $26 \pm 1^{\circ}\text{C}$ .

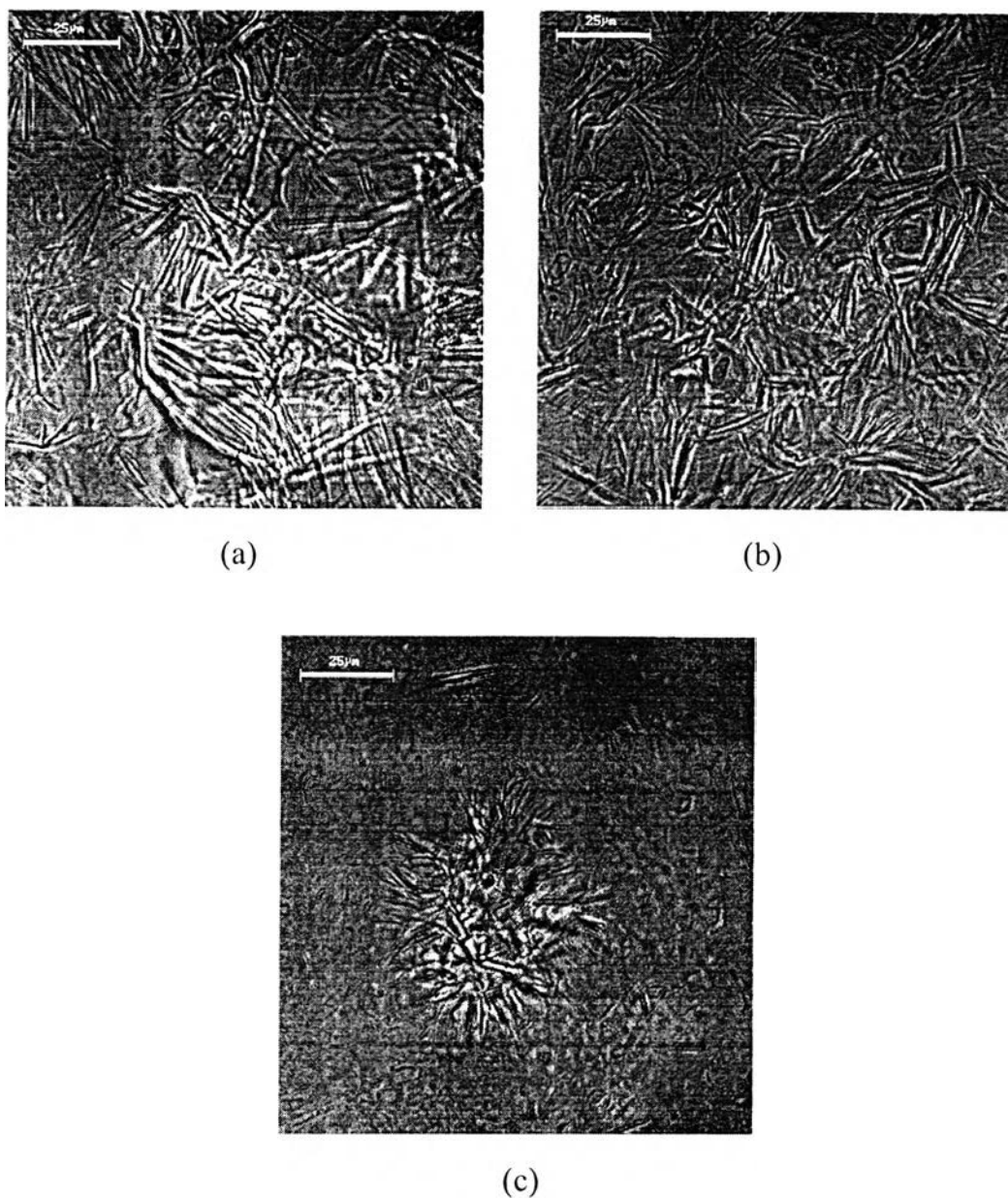


**Figure 4.27** Micrographs of emulsion obtained at 1000 magnification of MUC32:FA=1:2% by weight as a function of pH: (a) pH =5; (b) pH =7; (c) pH =10, and temperature was equal to  $26 \pm 1^{\circ}\text{C}$ .

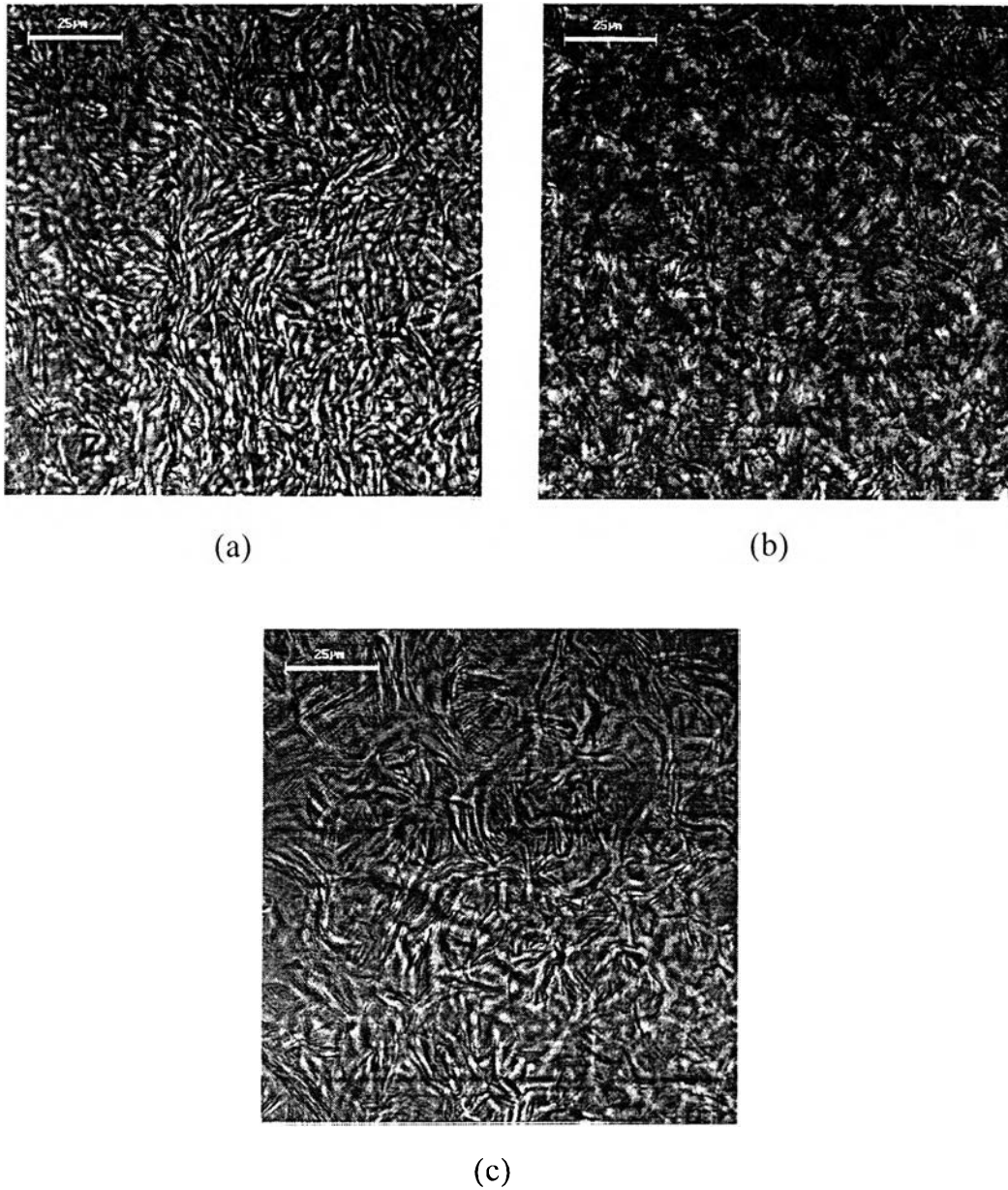


**Figure 4.28** Micrographs of emulsion obtained at 1000 magnification of MUC32:FA=1:4% by weight as a function of pH: (a) pH =5; (b) pH =7; (c) pH =10, and temperature was equal to  $26\pm 1^{\circ}\text{C}$ .

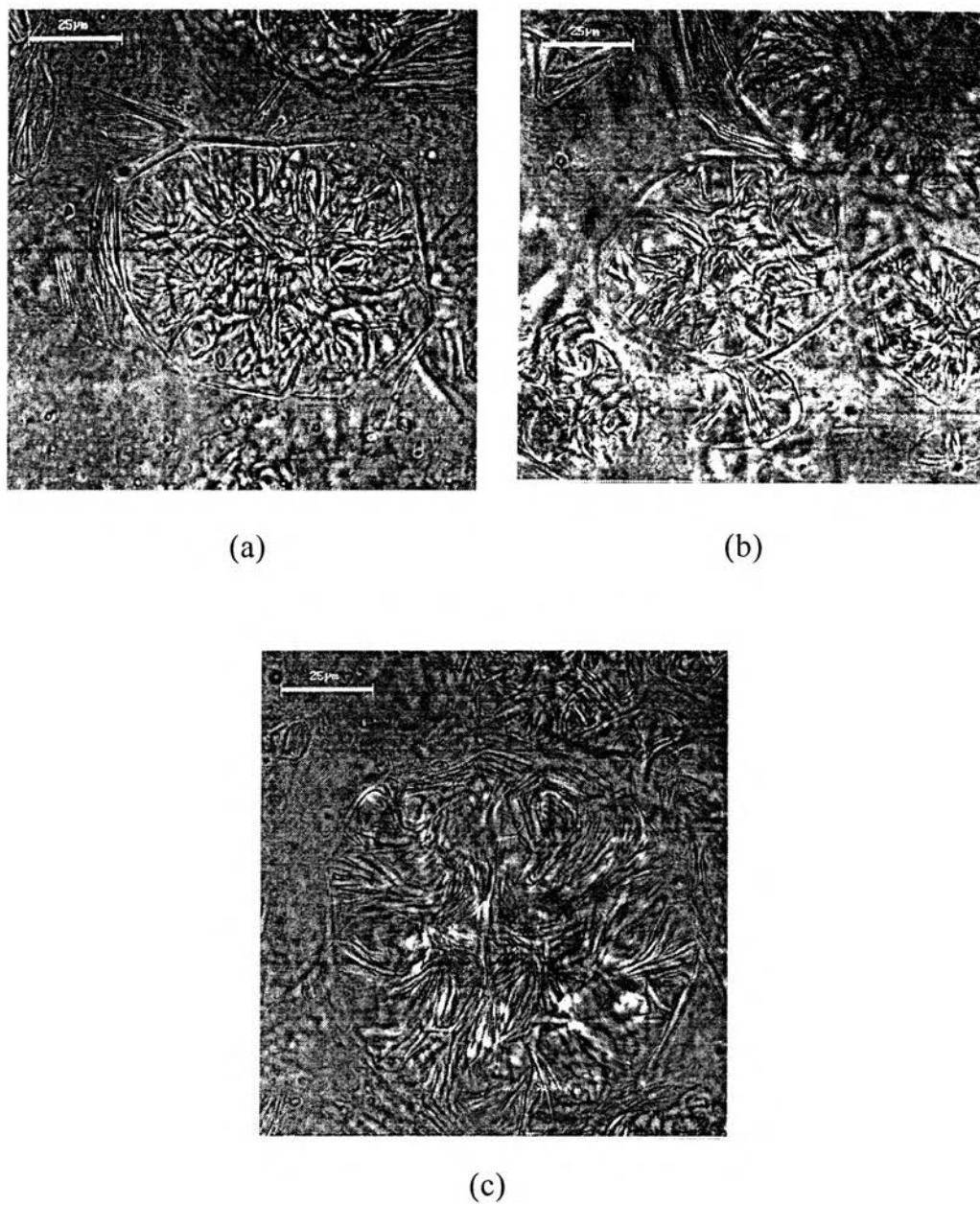


**Figure 4.29** Micrographs of emulsion obtained at 1000 magnification of MUC32:FA=1:6% by weight as a function of pH: (a) pH =5; (b) pH =7; (c) pH =10, and temperature was equal to  $26 \pm 1^{\circ}\text{C}$ .